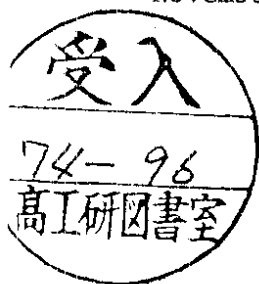


DEUTSCHES ELEKTRONEN-SYNCHROTRON **DESY**

DESY 74/56
November 1974



Lessons on e^+e^- Annihilation from Simple Chain Emission Models

by



N. S. Craigie

II. Institut für Theoretische Physik der Universität Hamburg

T. F. Walsh

Deutsches Elektronen-Synchrotron DESY, Hamburg

2 HAMBURG 52 · NOTKESTIEG 1

To be sure that your preprints are promptly included in the
HIGH ENERGY PHYSICS INDEX ,
send them to the following address (if possible by air mail) :

DESY
Bibliothek
2 Hamburg 52
Notkestieg: 1
Germany

Lessons on e^+e^- Annihilation from Simple Chain Emission Models

by

N.S. Craigie *

II. Institut für Theoretische Physik der Universität Hamburg

T.F. Walsh

Deutsches Elektronen-Synchrotron DESY, Hamburg

Abstract

The dearth of solvable models for e^+e^- annihilation often reduces one to excessively qualitative considerations, leaving obvious dynamical questions open. We discuss here various aspects of chain-emission models, which can be cast into solvable form. In such models the virtual photon decays into a link (a pion, for example) and some state (e.g. an off-shell vector meson) which decays by sequentially shedding further links.

Topics include the scaling behaviour in such models (including how it is broken near $\omega = 0$); neutral/charged distributions; the effect of internal quantum numbers and, in a particularly simple version of the model, the two-particle distributions. In particular, we show how a large neutral to charged energy ratio can arise. Finally, we discuss variants on such models arising from possible variety in the links of the chain, (i.e. multichannel effects), and also the nonlinear effects arising from the branching of a chain into chains.

* present address: Theory Division, CERN, Geneva.

It is customary to approach the dynamics of multiparticle production processes through the construction of models which embody definite physical pictures of the dynamics. Some time ago a vector meson resonance tree graph model was proposed in order to explain the multi-pion e^+e^- annihilation cross-sections in the low q^2 region (1). However this model lacked a suitable mathematical framework to extend it in a tractable way to larger q^2 . We shall discuss here a simplified version of this model, which can be described in terms of solvable equations and from which a number of detailed dynamical questions can be answered. With simple tractable models one can learn piecemeal about the physics; hopefully one can learn lessons which may apply in wide classes of models and might even reflect general features of a satisfactory theory of the dynamics in question. Ideally, models for e^+e^- annihilation should also apply to deep inelastic lepton-hadron phenomena; there is a widespread belief that the two classes of processes are related. On the other hand, we believe that it is useful to construct less ambitious models for e^+e^- processes alone. The present model may be able to shed some light on the continuation from timelike $Q^2 = s$ to spacelike Q^2 , but it is not with this aim that we discuss it.

We wish to describe here a class of models for e^+e^- annihilation based on the idea of chain emission. For example, the virtual photon is imagined to couple to a hadron system of low spin and isospin $I = 0$ and 1 . This system decays by emitting a hadron or hadron cluster (e.g. a pion or a meson resonance) and recoiling as a system of the same character but different mass. This process is repeated until the decay is complete and only stable mesons populate the final state. The essential feature which makes such a linear chain model tractable is the assumption that the hadron system remains in some sense the same during this decay process (we will make this more precise later). Restricting ourselves to the especially simple case of single pion emission, we can depict this decay as in Fig. 1. The hadron system which forms the backbone of this decay chain should be non-exotic ($I = 0, 1$ for pion emission) and should not make large excursions in spin in the course of the decay. We might mention here a nice lesson arising from the model with alternating $I = 0, 1$ states: the neutral to charged energy ratio can be large.

Further, we can imagine that transition to high spin systems is inhibited by angular momentum barriers. If for illustrative purposes we imagine the system to be a heavy vector state starting at large mass and $J = 1$ on a Chew-Frautschi plot, then this assumption amounts to saying that the system

cascades down in mass remaining near the $J = 1$ line as it emits mesons. The system can be either an on-shell state or one off its mass shell (e.g. a ρ_n meson with $p^2 = M_n^2$ or an off-shell ρ meson with $p^2 \gg m_\rho^2$). In most of this paper we shall make the simplest assumption possible: namely, that the system keeps fixed spin ($J = 1$ when we need spin properties); we shall see that relaxing this condition leads to some classic coupled-channel effects.

Remaining with our example, we can see that the hadron spectra in the final state depend on the way in which this hadron system migrates in mass on the Chew-Frautschi plot--in particular, it depends in the average jump length in mass per emitted hadron. We can imagine two extremes. In one, the hadron system jumps on the average a fixed or nearly fixed mass interval at each emission step. The final state hadrons then have large multiplicity and low momenta which do not grow or do not grow rapidly as the mass of the initial system is increased (though the mean momentum does not tend to remain constant for single particle emission on account of angular momentum effects /2/ (hereafter referred to as (I))). In the other extreme, we imagine that on the average the system makes a jump which is a fraction of the distance in M^2 separating it from the edge of the Chew-Frautschi plot. In this case the mean hadron momentum tends to grow with the mass of the initial system (the e^+e^- CM energy) and the multiplicities tend to grow slowly. A classification of these behaviors in a simple version of such models with fixed spin $J = 1$ has been given in I. We shall concentrate here on the second case, in which the model has a rich structure and for which we found the lessons from the model most interesting /3/ (hereafter referred to as II).

An important ingredient in the model--indeed, the one which turns the preceding remarks into a mathematically defined form -- is the assumption that there is an ordering on this linear chain so that on taking the cross section for Fig. 1 we get the integral equation corresponding to Fig. 2. On iteration, this generates "rainbow" diagrams without crossed links. We do not feel that relaxing this ordering assumption (analogous to that in the multiperipheral model) would change the physics in an essential way, though it would vastly complicate the analysis. With our assumption, we can do a great deal (see I and II). Considering $e^+e^- \rightarrow h + \text{anything}$, where "h" denotes the detected hadron, we can write an integral equation for the single particle distribution function in the form of Fig. 3 and also an equation in the form of Fig. 4 for the two particle distribution functions. All this holds for a chain with or

without spin; when we need spin properties we shall consider a "bare bones" model where the hadronic system keeps $J = 1$.

The equations of the model can be reduced to algebraic form by standard Mellin-transform methods. Choosing that solution corresponding to our picture of large jumps on a Chew-Frautschi plot, we find that the total e^+e^- annihilation cross section has a power behavior, the power being promoted over that for the terminal process $e^+e^- \rightarrow h_1 + h_2$ to s^α . As the CM energy $\rightarrow \infty$ for fixed non-zero $\omega = 2E_h/\sqrt{s}$, the single particle distributions scale in the variable ω (Feynman scaling). A significant lesson here lies in the fact that for small ω scaling is violated at any finite s . Moreover, the multiplicities in the model grow logarithmically in s , but the coefficient of this logarithmic growth is not given simply by integrating the asymptotic scaling function down to the lower kinematic limit $2m_h/\sqrt{s}$. This result seems quite general for such models and conflicts with a very popular bit of folklore. The model allows one to study sum rules for the moments in ω of the structure function and thus to study, for example, the way in which the cross section approaches its asymptotic form. For further details we refer the reader to II.

Some of the most interesting lessons from the model concern its isospin structure and the distributions of neutral and charged particles. The simplest version (our "bare bones" model with $I = 0$ oder $I = 1$) would correspond to pion emission with alternating isospins along the chain (ρ -like and ω -like states). Since the photon is usually assumed dominantly isovector in character, the initial transition of a heavy isovector state to a pion and an isoscalar state leads to a neutral pion carrying off a large fraction of the CM energy. By using the energy conservation sum rule we can find an expression for the ratio of the energy carried off by neutral pions to that carried off by charged pions in this simple model. This ratio can be as large as two in such models; put differently, the slopes of neutral and charged pion spectra can be dramatically different. A related lesson is that without special effort, such models as give a ratio of the number of neutral to charged pions equal asymptotically to $1/2$ only approach this value logarithmically (i.e. as $1/\langle N \rangle$). It is also possible to discuss neutral/charged correlations (e.g. the mean number of neutrals for fixed numbers of charged particles) and SU_3 in the context of such models.

Different models which give Feynman scaling asymptotically for single particle distributions can give quite different results for two-particle correlations. For this reason we consider the latter quite important. We discuss this in terms of the bare bones model with spin and isospin. Particularly nice features arise when we insist that of the two detected hadrons, one be fast ($\omega_1 \rightarrow 1$). The distribution of the second detected particle is given in terms of the single particle inclusive distribution; it is possible to determine the normality of the system recoiling against the fast hadron; finally, we note that the model has no transverse momentum cutoff. This is unlike the situation in parton models.

Our main aim in this work has been pedagogical. For this reason we have confined most of our concrete discussion to the bare bones model already mentioned: a $J = 1$ chain with pion emission and alternating isospins (ρ , ω -like states), leaving out either spin or isospin or both when inclusion of such effects would clutter the discussion to no advantage. Nevertheless, we would like to emphasize that our horizon is broader. We believe that such models can be extended to include radiation of particles other than pions (or pseudoscalar mesons in the SU_3 versions) and to allow for some migration in spin of the hadronic system in the course of the chain decay. We shall also consider the role played by non-linear terms in the cascade, which we shall show to have a unitarizing effect in the model.

In the next section we discuss the model divested even of the complexities of spin and isospin. This exhibits the dynamical features clearly. We shall comment on the case with spin. The added complexities of isospin and SU_3 are discussed in Sec. III along with the attendant effects on neutral/charged distributions. In Sect. IV we start to relax the condition that there be only one hadron system along the decay chain by studying a simple variation with two different types of decaying states in the context of a model without spin. In Sec. V, we face up to the full complexities of spin and isospin in a case where it has most to teach us: two particle inclusive distributions. We also discuss there the effects of the isospin structure of the bare bones model on two particle correlations. Finally in Sect. VI we shall consider what happens when one adds multi-pronged tree graph contributions to the cascade, which lead to non-linear terms in the basic equations describing the chain emission or cascade mechanism.

II. Basic Dynamics of the Model

1. We have already described the model in a qualitative way. In this section we shall obtain the equations of a particularly simple version. This will enable us to discuss the physical features of chain emission models with a minimum of technical encumbrances. The rest of the paper will consist of elaborations on the bare bones model. The essential lessons on the dynamics remain the same as in this section. We shall repeat here many of the points of paper II, to which we refer the reader for technical details on the model with spin.

The photon spin and isospin is ignored here and we suppose that the hadron system decays into only one type of particle. The decay chain for the emission of n -particles is shown in Fig. 1. The coupling of the photon to the initial hadron system can be absorbed into the definitions of the vertices and we shall not indicate it explicitly. Two types of vertices enter: one for the radiation of a single particle and one for the terminal decay into two particles. The precise form of this last link plays no essential role.

2. We will from now on consider not the cross section for $e^+e^- \rightarrow$ hadrons but rather the absorptive part of the scalar current correlation function,

$$\rho(s) = (2\pi)^4 \sum_H |\langle H | J(0) | 0 \rangle|^2 \delta(Q - P_H) \quad (2.1)$$

Summing up the contribution of Fig. 1 to $\rho(s)$, using the ordering principle mentioned in the introduction, we arrive at the integral equation depicted in Fig. 2; this generates rainbow diagrams on iteration. Writing $\langle p_1 p_2 | j(0) | 0 \rangle = f(s)$, the first term contributes $p |f|^2 / 4\pi\sqrt{s}$. The second involves the radiation vertex $\langle k; H - k | j(0) | 0 \rangle = 4\pi g(s, s') \langle H, -k | j(0) | 0 \rangle$ where $s = Q^2$, $s' = (Q-k)^2$. Both f and g are understood to contain the outermost propagator and the coupling to the photon if the hadron system is thought of as an off-shell single particle state (a restriction we do not need to make). The integral equation is easily worked out to be (we ignore masses throughout)

$$\rho(s) = \rho_0(s) + \lambda \int_0^1 d\eta K(s, \eta s) \rho(\eta s) \quad (2.2)$$

where $\eta = s'/s$, λ is for later convenience and

$$K(s, s') = (1-\eta)s |g(s, s')|^2 = (1-\eta)h(s, \eta s)$$

The inclusion of spin would change the precise form of K , but nothing else. Of course, we would then have to deal with two structure functions for the once-inclusive reaction. Physically, K represents the probability that a system of squared mass s will decay into one of squared mass s' .

3. We can now proceed to the single particle inclusive reaction $e^+e^- \rightarrow h + \text{anything}$. If we hold one momentum fixed and sum over all others then the corresponding integral equation is that shown in Fig. 3. The differential structure function is defined by

$$d\rho(s,p) = \sum_H (2\pi)^4 |\langle H,p | j(0) | 0 \rangle|^2 \delta(Q-p-p_H) \frac{d^3\phi}{(2\pi)^3 2E} \quad (2.3)$$

The first term is just the product of the vertex squared and the function ρ at $s' = (1-\omega)s$, where $\omega = 2p \cdot Q/s = 2Eh/\sqrt{s}$ ($Q^2 = s$) is the scaling variable for the detected particle. The second term is more involved. As in (2.2), a phase space integral over $\eta = s'/s$ appears; in addition there is an integration over the relative angle of \underline{p} and \underline{k} . This played no role in (2.2). After changing variables to $\omega' = 2p \cdot (Q-k)/s'^2$ and paying close attention to the limits of integration, one finds $F(s,\omega) = d\rho/d\omega$ satisfies the integral equation

$$F(s,\omega) = F_0(s,\omega) + \lambda \int_{\omega}^1 \frac{d\omega'}{\omega} \frac{\omega'}{\omega} \int_{\omega'}^{\omega'/\omega} d\eta \eta \cdot h(s,\eta s) F(\eta s, \omega') \quad (2.4)$$

where

$$F_0(s,\omega) = 4 \omega h(s, (1-\omega)s) \rho((1-\omega)s)$$

4. The above complications are present in increased degree in the equation for the two-particle inclusive distributions in $e^+e^- \rightarrow p_1 + p_2 + \text{anything}$. One can check that iteration of the equation depicted in Fig. 4 generates the correct set of rainbow diagrams. The relevant invariants are now $\omega_1 = 2p_1 \cdot Q/Q^2$, $\omega_2 = 2p_2 \cdot Q/Q^2$ and $\eta_{12} = (p_1 + p_2)^2/Q^2$. The equation for the two particle distribution function $H(s, \omega_1, \omega_2, \eta_{12})$ is

$$\begin{aligned}
H(s, \omega_1, \omega_2, \eta_{12}) &= H_o^{(1)} + H_o^{(2)} \\
&+ \lambda \int \frac{d\omega_1'}{\omega_1} \frac{\omega_1'}{\omega_1} \int \frac{d\omega_2'}{\omega_2} \frac{\omega_2'}{\omega_2} \int d\eta \eta \Lambda^{-1/2} \theta(\Lambda) h(s, \eta s) \times \\
&\times H(\eta s, \omega_1', \omega_2', \eta_{12})
\end{aligned} \tag{2.5}$$

where

$$H_o^{(1)} = \lambda h(s, (1-\omega_1)s) F((1-\omega_1)s, \omega_2)$$

$$H_o^{(2)} = \lambda h(s, (1-\omega_2)s) F((1-\omega_2)s, \omega_1)$$

$$\Lambda = \det \begin{vmatrix} 2 & 1+\eta & \omega_1 & \omega_2 \\ 1+\eta & 2\eta & \omega_1' & \omega_2' \\ \omega_1 & \omega_1' & 0 & \eta_{12} \\ \omega_2 & \omega_2' & \eta_{12} & 0 \end{vmatrix} \tag{2.6}$$

5. The solutions to these equations depend on the behavior of the vertex $h(s, \eta s)$. The model so far is general and can incorporate different behaviors for this vertex. For the sake of definiteness we want to concentrate here on the case where the vertex scales,

$$h(s, \eta s) = h(\eta) \tag{2.7}$$

and is a function of η alone. This is certainly the simplest choice for the dimensionless function $h(s, \eta s)$: it depends only on the dimensionless ratio η . We shall see that this leads to scaling in ω for the structure function $F(s, \omega)$. The assumption (2.7) has a simple physical interpretation. It corresponds to long jumps on the Chew-Frautschi plot of finite mean length in dimensionless units, independent of the value of s with which one starts the decay of the hadronic system.

Substituting (2.7) into (2.2) and (2.4) and defining the Mellin transforms

$$\begin{aligned}\hat{\rho}(j) &= \int_1^{\infty} ds s^{-1-j} \rho(s) \\ \hat{F}(j, \xi) &= \int_1^{\infty} ds s^{-1-j} \int_0^1 d\omega \omega^{-1+\xi} F(s, \omega)\end{aligned}\tag{2.8}$$

we have for $\hat{\rho}(j)$,

$$\begin{aligned}\hat{\rho}(j) &= \frac{1}{1-\lambda K(j)} \hat{\rho}_0(j) \\ K(j) &= \int_0^1 d\eta \eta^j (1-\eta) h(\eta)\end{aligned}\tag{2.9}$$

The asymptotic behavior of $\rho(s)$ is determined by the largest $j = \alpha(\lambda)$ for which $1-\lambda K(\alpha(\lambda)) = 0$, in which case

$$\rho(s) \underset{s \rightarrow \infty}{\sim} \rho_0(\alpha) \lambda \frac{\partial \alpha}{\partial \lambda} s^{\alpha(\lambda)}\tag{2.10}$$

Since $h(\eta)$ is not known, it is difficult to say anything about the power $\alpha(\lambda)$. Of course, we have assumed that α leads the singularity of $\hat{\rho}_0$. Otherwise ρ would have the same s -dependence as ρ_0 . It is well known that in the case with spin (where $\sigma(s) \sim s^{-1} \rho(s)$) an increasing $\rho(s)$ is not compatible asymptotically ($s \gtrsim 4 \times 10^4 \text{ GeV}^2$!) with one-photon e^+e^- annihilation (4), and even causes problems for QED at high but attainable energies (5). This is really an experimental question, and we merely note that it may be interesting and useful to imagine models where the large s behavior of $\rho(s)$ is not constrained, and in which the dynamical origin of the energy dependence can be traced out - at least in principle.

6. Proceeding similarly with $F(s, \omega)$ we have (6)

$$\begin{aligned}\hat{F}(j, \xi) &= \frac{1}{1-\lambda \Phi(j, \xi)} \hat{F}_0(j, \xi) \\ \Phi(j, \xi) &= \int_0^1 d\eta \eta^{j+1} \frac{1-\eta \xi^{-2}}{\xi^{-2}} h(\eta)\end{aligned}\tag{2.11}$$

The Mellin transform of $F_0(s, \omega)$ factorizes

$$\hat{F}_0(j, \xi) = \hat{\rho}(j) H(j, \xi) \quad (2.12)$$

where $H(j, \xi)$ does not interest us here; it has singularities only in the left half plane for both j and ξ , and it decreases in the right half plane. Now, (2.11) will have a pole at $j = \alpha(\lambda)$ and in the limit $s \rightarrow \infty$ and ω fixed and non-zero this will lead to a factorization of $F(s, \omega)$. Namely

$$F(s, \omega) \sim s^{\alpha(\lambda)} f(\omega) \quad (2.13)$$

$$f(\omega) = \int_{c-i\infty}^{c+i\infty} \frac{d\xi}{2\pi i} \omega^{-\xi} \frac{H(\alpha, \xi)}{1 - \lambda \Phi(\alpha, \xi)}$$

In other words, the model leads to scaling in the variable ω . This follows, of course, only so long as the singularities of $(1 - \lambda \Phi(j, \xi))^{-1}$ lie to the left of $\alpha(\lambda)$. This is the case for $\omega \neq 0$, as is most easily seen by noting that a singularity to the right of $\alpha(\lambda)$ for $\hat{F}(j, \xi)$ would, by integrating the energy sum rule (2.14a).

$$2 \rho(s) = \int d\omega \omega F(s, \omega) \quad (2.14a)$$

produce a contribution to $\rho(s)$ growing faster than s^α ; the multiplicity is given by the sum rule

$$\langle n \rangle \rho(s) = \int d\omega F(s; \omega) \quad (2.14b)$$

For $\omega = 0$, inspection of (2.11) shows that $1 - \lambda \Phi(j, 1) = 1 - \lambda K(j)$ so that the integrand develops a simple pole at $\xi = 1$. This singularity leads to $f(\omega) \sim \omega^{-1}$ as $\omega \rightarrow 0$, with a coefficient proportional to $(\partial \Phi / \partial \xi)^{-1}$. If we integrate this singular scaling function down to the kinematic minimum $2m/\sqrt{s}$ in the expression (2.14b) with $F(s, \omega)$ replaced by $s^\alpha f(\omega)$, we would get a logarithmic increasing multiplicity with the coefficient proportional to $(\partial \Phi / \partial \xi)^{-1}$. The multiplicity is in fact logarithmic and is given exactly by (2.15a):

$$\langle n \rangle \rho(s) = \lambda \frac{\partial}{\partial \lambda} c(s) \quad (2.15a)$$

$$\langle n^2 \rangle \rho(s) = \left(\lambda \frac{\partial}{\partial \lambda} \right)^2 \rho(s) \quad (2.15b)$$

where $\rho(s)$ is an implicit function of λ through $\alpha(\lambda)$.

Inserting the asymptotic behavior of $\rho(s)$ we find

$$\langle n \rangle = \lambda \frac{\partial \alpha}{\partial \lambda} \ln s + \dots$$

Using $\lambda \frac{\partial \alpha}{\partial \lambda} = -(\lambda \frac{\partial K(\alpha)}{\partial \alpha})^{-1}$ and equations (2.9) and (2.11) we see that the coefficient of the ω^{-1} term in $f(\omega)$ and the coefficient of the exact expression for the multiplicity are in general unrelated to one another. Physically, this is because $f(\omega)$ contains a singularity not present in $F(s, \omega)$, which vanishes at the lower kinematic limit for any finite s . The multiplicity is built up by the rapid increase of $F(s, \omega)$ at smaller and smaller values of ω as s increases. The progressive development of this singularity continues even after scaling has been established at any finite ω . The result is that one cannot interchange the scaling limit and the integral in (2.14b), and to the conclusion already mentioned. This comment should apply to all chain-emission models, and indicates that in any scaling model with increasing multiplicity one has to be careful in discussing the multiplicity sum rule; see II).

7. The singularity which appears in the integrand of (2.13) can be exhibited in another way by using the energy sum rule (2.14a) and carrying out the ξ integration. Since $H(j, \xi)$ decreases in the right half plane, we can pick up the pole in ξ generated by this integration to find

$$2\rho(s) = \int_{c-i\infty}^{c+i\infty} \frac{dj}{2\pi i} s^j \frac{\hat{\rho}(j) H(j, 2)}{1 - \lambda \Phi(j, 2)} \quad (2.16)$$

Since the singularity of $(1 - \lambda \Phi(j, 2))^{-1}$ lies to the left of that in $\rho(j)$, it contributes the non-leading term to $\rho(s)$; some algebra suffices to show that the coefficient for this term is negative. That is, the cross section approaches its asymptotic limit for below.

From the preceding discussion it is evident that the scaling behavior is broken for small ω , since this is where the singularity in $f(\omega)$ is being built up as s increases. For any finite s , we expect $F(s,\omega)$ to rise from zero at $\omega = 2m/\sqrt{s}$, reach a maximum at some ω and then decrease toward $\omega = 1$. This maximum steadily increases in height with s and moves to smaller and smaller ω , so that the region in ω for which $F(s,\omega)$ scales increases with s . For some qualitative pictures we refer to II. We should note here that a breaking of scaling for small ω and finite energies emerges from quite different approaches and is probably a feature of any model of e^+e^- annihilation (7,8,9).

8. The behavior as $\omega \rightarrow 1$ is of considerable interest. From (2.13) we see that at $\omega = 1$, $f(1) = 0$; the rate of decrease as $\omega \rightarrow 1$ is determined by how rapidly $H(j,\xi)$ decreases as $\xi \rightarrow \infty$ in the right half plane. This corresponds to the simple observation that as $\omega \rightarrow 1$ only the driving term survives. An interesting feature of the bare bones model with spin is that as $\omega \rightarrow 1$ the transversality of the coupling (it has the spin structure of the $\rho \omega \pi$ vertex (II) asserts itself, leading to

$$\bar{W}_L / \bar{W}_T \xrightarrow{\omega \rightarrow 1} O((1-\omega)^2) \quad (2.17)$$

where \bar{W}_L and \bar{W}_T are the conventional longitudinal and transverse structure functions for the once inclusive process. A very similar point will recur in Section V.

III. Multiplicities and Internal Symmetries

1. So far we have studied some dynamical features of chain-emission models. Most of what we have to say in this section is based on the isospin structure of the bare bones model. For some of this discussion it would be useful if we could make some statement about the dispersion $\langle n^2 \rangle - \langle n \rangle^2$ or equivalently about $f_2 = \langle n(n-1) \rangle - \langle n \rangle^2$, since it is interesting to see whether the distribution is broader or narrower than a Poission ($f_2 > 0$ or < 0). From (2.15) we can calculate the dispersion which, up to terms increasing as $\ln s$ is (I)

$$\langle n^2 \rangle - \langle n \rangle^2 = \langle n \rangle + \lambda^2 \frac{\partial^2 \alpha}{\partial \lambda^2} \ln s \quad (3.1)$$

where $K^{(n)} = \partial^n K / \partial \alpha^n$

$$\lambda^2 \frac{\partial^2 \alpha}{\partial \lambda^2} = \frac{1}{\lambda K'} \frac{1}{(K')^2} (2(K')^2 - K K'')$$

One can readily verify that $K' < 0$ (see Sect. II) and $K'' > 0$, so that the distribution is narrower or broader than Poission depending on whether $2(K')^2 - K K''$ is positive or negative. For small λ we expect $\lambda^2 \partial^2 \alpha / \partial \lambda^2$ to be small compared to the coefficient of $\langle n \rangle$, $\lambda \partial \alpha / \partial \lambda$ so that the distribution is approximately Poission. As for the large λ limit, we just mention that for a simple example with $h(\eta) = \text{const}$ one has a distribution which becomes narrower than Poission for large λ .

2. There are numerous interesting features to the bare bones model with isospin. One of these is the ratio of the numbers of neutral and charged pions. It is well known that for an isoscalar photon of odd charge conjugation this ratio ($n_c \equiv n_{\pi^+} + n_{\pi^-}$) is $\langle n_o \rangle / \langle n_c \rangle = 1/2$ averaged over all charge configurations at fixed N (a recent discussion with references: Ref. (10)). We can use this to find $\langle n_o \rangle / \langle n_c \rangle$ for an even number of pions $N = \langle n_o \rangle + \langle n_c \rangle$ so long as we use the bare bones model. This is because an isovector photon, after radiating a single neutral pion, gives rise to an $I = 0$ hadronic system. This decay then yields $\langle n_o \rangle / \langle n_c \rangle = 1/2$ and it is easy to see that for even N , $\langle n_o \rangle / \langle n_c \rangle = (N+2)/(2N-2)$ and, taking account of the expected 3:1 isovector: isoscalar ratio we have (now averaged over N)

$$\frac{\langle n_o \rangle}{\langle n_c \rangle} = \frac{2\langle N \rangle + 3}{4\langle N \rangle - 3} \quad (3.2)$$

Of course, we have implicitly assumed that $\langle N \rangle$ is large and the distribution broad. Otherwise the N variation produced by the isovector:isoscalar ratio would cause (3.2) to oscillate as $\langle N \rangle$ increases.

What appears significant to us is that $\langle n_o \rangle / \langle n_c \rangle$ approaches its expected asymptotic value of $1/2$ only as $1/\langle N \rangle \sim (\ln s)^{-1}$. A more rapid approach to the limit would require a more complicated isospin structure, at least in the context of chain-emission models. It is perhaps worth mentioning that we expect more general chain emission models to yield $\langle n_o \rangle / \langle n_c \rangle \rightarrow 1/2$ as $s \rightarrow \infty$, so long as the radiated particles and those along the chain have conventional isospin and do not have isospin violating decays. The situation is quite different when we treat the ratio of the energies carried off by neutral and charged pions, as we shall do next.

3. More interesting than $\langle n_o \rangle / \langle n_c \rangle$ in our bare bones model is the ratio of neutral to charged energies. This is also what is most easily inferred from experiment. Just as in our preceding argument, where the enhancement of $\langle n_o \rangle / \langle n_c \rangle$ above $1/2$ came from the first π^0 radiated along the chain (for an isovector photon), so here the only source of asymmetry in the energy distribution among neutral and charged pions arises from the first radiated π^0 . The entire effect is then due to the fact that in the model with alternating isospins the isovector photon must dispose of its isospin by emitting a π^0 before it can give rise to an $I = 0$ recoil system. Let the first π^0 carry off a fraction $\sqrt{s}/2(1-\bar{\eta})$ of the CM energy as $s \rightarrow \infty$. It is easy to convince oneself that the remaining pions recoiling against this first one share the remaining energy equally, so that $\langle E_c \rangle = 1/3 \sqrt{s} (1+\bar{\eta})$. Then we have $\langle E_o \rangle = 1/2\sqrt{s}(1-\bar{\eta}) + 1/6\sqrt{s}(1+\bar{\eta})$ and

$$\frac{1}{2} \leq \left(\frac{\langle E_o \rangle}{\langle E_c \rangle} \right)_{I_\gamma=1} = \frac{2 - \bar{\eta}}{1 + \bar{\eta}} \leq 2 \quad (3.3)$$

This argument can easily be made more precise. In fact, we can obtain an expression for $\bar{\eta}$. First, note that the above argument corresponds directly to the

decomposition of Fig. 3 for an isovector photon. The first term on the right in the figure is driving term in the integral equation, F_0^α (α is the charge index), and the second we shall call F_{int}^α . Clearly F_0^α vanishes unless $\alpha = 0$; F_{int}^α is independent of α . We now take over the normalization for the case with spin(II), as we wish to make a numerical estimate. Now the energy sum rule reads (note the definition of F)

$$\sum_{\alpha} \frac{1}{2(4\pi)^2} \frac{1}{\rho} \int_0^1 d\omega \omega^2 (F_0 + 3F_{int}) = 1 \quad (3.4)$$

From this we can express the integral over F_{int} in terms of that over F_0 ; but the latter is known. In the spin 1 case it is

$$F_0 = (4\pi)^2 \lambda \omega^2 (1-\omega) h(1-\omega) \rho((1-\omega)s)$$

and so

$$\frac{1}{(4\pi)^2} \frac{1}{\rho} \int_0^1 d\omega \omega^2 F_0(s, \omega) = \frac{1}{2} [1 - \lambda \int_0^1 d\eta \eta^{2+\alpha} (1-\eta)^3 h(\eta)] \quad (3.5)$$

Finally, we have

$$\frac{1}{2(4\pi)^2} \frac{1}{\rho} \int_0^1 d\omega \omega^2 F_{int} = \frac{1}{6} (1 + \bar{\eta}) \quad (3.6)$$

$$\bar{\eta} = \frac{\int_0^1 d\eta \eta^{2+\alpha} (1-\eta)^3 h(\eta)}{\int_0^1 d\eta \eta^{1+\alpha} (1-\eta)^3 h(\eta)}$$

The extra $(1-\eta)^3$ in (3.6) is due to extra momentum factors arising from the " $\rho\omega\pi$ " vertex in the case with spin.

Just as an example, take $h = \text{const.}$; then $\bar{\eta} = (2+\alpha)/(6+\alpha) \sim \frac{3}{7}$ for $\alpha \sim 1$ (i.e. ρ rising linearly with s). Again including an isoscalar contribution of $1/3$ the isovector we get $\langle E_0 \rangle / \langle E_c \rangle \sim .9$. Of course, this is only a crude guess since we really know nothing about $h(\eta)$; however, $\bar{\eta} < 1$ in general.

It needs to be emphasized that in this model $\langle E_o \rangle / \langle E_c \rangle$ is energy independent once the energy is high enough so that Feynman scaling is established and $\bar{\eta}$ is energy independent. $\langle E_o \rangle / \langle E_c \rangle$ cannot rise indefinitely. From our discussion of the bare bones model, this is clearly a general feature.

4. We now see that in chain-emission models the behavior of π^0 and π^+ spectra can be quite unlike. In the simple model we have been discussing we expect a substantial difference which reaches a maximum in the vicinity of $\omega \sim \bar{\eta}$. At low energies this might simply appear as a π^0 momentum distribution which is flatter than that for charged pions. At high energies one should see a hump in $F^{\pi^0} - F^{\pi^+}$. Also note that as $\omega \rightarrow 1$ the driving term dominates so that

$$\lim_{\omega \rightarrow 1} F_{I_Y=1}^{\pi^+} / F_{I_Y=1}^{\pi^0} \rightarrow 0 \quad (3.7)$$

There is a well-known relation in the quark parton model, $F^{\pi^0} = F^{\pi^+}$ (10). This arises because in the t-channel of the process $\gamma\pi^\alpha \rightarrow \gamma\pi^\alpha$ (one of whose discontinuities gives F^α) only $q\bar{q}$ states of $I \leq 1$ can appear. In chain-emission models there is no such constraint, one can have $I = 2$ and $F^{\pi^0} \neq F^{\pi^+}$ in general. Put differently, the difference arises because the fragmenting states are octets and not triplets as in the quark parton model. If one regards this feature of the bare bones model with distaste and, out of regard for conventional dual ideas, imposes $I \leq 1$ and $F^{\pi^0} = F^{\pi^+}$, the chain must be more complicated and involve A_2 -like states. The isospin can then no longer alternate as in our bare bones model.

We want to emphasize that the observation of a large F^{π^0} / F^{π^+} ratio at $\omega \neq 0$ has strong implications for the isospin structure of the chain in any model of this type; the bare bones model offers an explicit lesson on this point.

5. A considerable advantage to chain-emission models is their similarity to models already familiar in hadronic processes. We want to consider here the neutral/charged correlations for the bare bones model, where the situation is particularly transparent. We can then see qualitatively how more general chain-emission models will behave from their hadronic analogues. The distribution of neutral and charged pions is $(N = n_o + n_c)$ (11)

$$P(n_o, n_c) = P_N \Gamma(n_o, n_c) \quad (3.8)$$

where P_N is the probability to produce N pions and Γ is the "branching ratio" of this state into n_o neutral and n_c charged pions. The above are normalized by

$$\sum P_N = 1$$

$$\sum_{\substack{n_o, n_c \\ n_o + n_c = N}} \Gamma(n_o, n_c) = 1$$

It is easy to separate N even (isovector photon) and N odd (isoscalar photon) so as to take account of the isovector/isoscalar ration, and we won't do this explicitly. Two useful quantities are the probability to produce n_c charged particles, summed over neutrals, and the mean number of neutrals given that the number of charged particles is fixed,

$$P(n_c) = \sum_{n_o} P(n_o, n_c) \quad (3.9)$$

$$\langle n_o \rangle_{n_c} P(n_c) = \sum_{n_o} n_o P(n_o, n_c)$$

Clearly, the physics lies in P_N and $\Gamma(n_o, n_c)$. P_N depends on the detailed dynamics of the model; $\Gamma(n_o, n_c)$ depends on the isospin structure of the chain, as we can demonstrate by considering the bare bones model.

We can calculate Γ by noting that the last three pions on the chain always consist of two charged and one neutral. A ρ -like state elsewhere in the chain gives (in pairs) $\pi^0\pi^0$, $\pi^+\pi^-$ and $\pi^-\pi^+$ with equal probability. The number of such ρ -like links (except the last) is

$$m = \frac{N-4}{2} \quad N \text{ even}$$

$$m = \frac{N-1}{2} \quad N \text{ odd}$$

Writing the number of charged pions as $n_c = 2 + 2k$ ($k = 0, 1, \dots$) a straightforward combinatoric argument gives

$$\Gamma(n_o, n_c) = \left(\frac{1}{3}\right)^{m-k} \left(\frac{2}{3}\right)^k \frac{m!}{k!(m-k)!} \quad (3.10)$$

- i.e. we have a binomial distribution by pairs of charged particles. In obtaining this, we have ignored the channel with only two charged pions. Because of the decreasing pion form factor this channel should be ignorable.

From (3.9) and (3.10) we can calculate $P(n_c)$ and $\langle n_o \rangle_{n_c}$ - if P_N is known. Since it is not, we shall just make some comments, ignoring the question of the isovector/isoscalar ratio.

- (i) If P_N is a Poisson, then the binomial character of $\Gamma(n_o, n_c)$ leads to $P(n_c)$ also being a Poisson distribution and $\langle n_o \rangle_{n_c} = \langle n_o \rangle$. Even if $\Gamma(n_o, n_c)$ is binomial only in pairs, one arrives at the approximate equality $\langle n_o \rangle_{n_c} = \langle n_o \rangle$.
- (ii) If P_N is much narrower or broader than a Poisson, then correspondingly $P(n_c)$ is also. This need not be the case in general. In fact the situation is quite different, when collective effects play a role (e.g. when the isospin bounds are saturated or nearly saturated (12)). For the chain model distribution much narrower than a Poisson leads to $\langle n_o \rangle_{n_c}$ decreasing as n_c increases, because $n_o + n_c = N = \langle N \rangle$ (for a narrow distribution) On the other for broad distributions $\langle n_o \rangle_{n_c}$ tends to increase as n_c increases (II).

Of course, this only holds if Γ is binomial or approximately so. If the radiated particles are meson resonances or clusters, then the presence of such clustering is reflected in the behavior of, e.g., $\langle n_o \rangle_{n_c}$ which then tends to rise as a function of n_c even for a Poisson distribution. The variety of behaviors possible indicates that it is of some importance to try to separate P_N and $\Gamma(n_o, n_c)$. This may be difficult experimentally, but it is necessary if one is to disentangle the dynamical and isospin structure arising from any model - not just chain emission models.

6. There is no dimensional scale in the model (such as the p_T cutoff in the parton model), so it may be that at very high energies the production of heavy particles is not disfavored. This makes it interesting to consider the model with SU_3 included. We shall do this for the simple case where one has an octet electromagnetic current and pure octet hadron states, including both the radiated particles (the pseudoscalar octet) and the chain states (C = - vector-meson octet-like states). The current propagator is diagonal in the SU_3 indices and we can take the radiation vertex to be pure D-type, the driving term in Fig. 3 now being F-type. For the driving term in the inclusive structure functions we will have a D-type coupling. For the notation we refer to Ref. (13).

There are now eight $\hat{\rho}_a(j)$, $a = 1, \dots, 8$. We shall need to solve for $\hat{\rho}_{em} = \hat{\rho}_3 + \frac{1}{3} \hat{\rho}_8$, given the usual SU_3 classification of the electromagnetic current (13). The $\hat{\rho}_a$ satisfy the algebraic equation

$$\hat{\rho}_a = \hat{\rho}_{oa} + \lambda \sum_b K_{ab} \rho_b \quad (3.11)$$

where

$$\begin{aligned} \hat{\rho}_{oa}(j) &= \sum_{rs} (f_{ars})^2 \hat{\rho}_a(j) = 3 \hat{\rho}_o(j) \\ K(j)_{ab} &= \sum_r (d_{arb})^2 K_o(j) \end{aligned} \quad (3.12)$$

Writing these equations out, we see by inspection that

$$\begin{aligned} \hat{\rho}_1 &= \hat{\rho}_2 = \hat{\rho}_3 \\ \hat{\rho}_4 &= \hat{\rho}_5 ; \hat{\rho}_6 = \hat{\rho}_7 \end{aligned}$$

After which one is left with three equations

$$\begin{aligned} (8\lambda K_o + 3) \hat{\rho}_3 + (2\lambda K_o - 9) \hat{\rho}_8 &= -18 \hat{\rho}_o \\ (8\lambda K_o + 3) \hat{\rho}_3 + (7\lambda K_o - 12) \hat{\rho}_6 &= -27 \hat{\rho}_o \\ (\lambda K_o - 3) \rho_3 + 3\lambda K_o \hat{\rho}_6 + \lambda K_o \hat{\rho}_8 &= -9 \hat{\rho}_o \end{aligned} \quad (3.13)$$

which can be solved without trouble to yield

$$\hat{\rho}_3(j) = \hat{\rho}_6(j) = \hat{\rho}_8(j) = \frac{9 \hat{\rho}_0(j)}{3-5\lambda K_0(j)} \quad (3.14)$$

The solution for the Mellin transformed current-correlation function is then just

$$\hat{\rho}_{em}(j) = \frac{4 \hat{\rho}_0(j)}{1-\lambda \frac{5}{3} K_0(j)} \quad (3.15)$$

which involves nothing more than a rescaling of λ and $\hat{\rho}_0$, and only changes the eigenvalue equation for $\alpha(\lambda)$.

7. Incorporating SU_3 for the inclusive structure functions is a bit more involved. For now we just note that by the same method as above we have for a current of index γ an inclusive structure function F_γ^α to radiate a particle of type a and

$$\hat{F}_\gamma^a(j, \xi) = c_\gamma^a \hat{F}_0(j, \xi) + \lambda \sum_b c_\gamma^b \hat{F}_b^a(j, \xi) \phi(j, \xi) \quad (3.16)$$

where

$$c_\gamma^a = \sum_b (d_{a\gamma b})^2$$

Quite independent of any model we expect the U-spin relation $F^{\pi^+} = F^{K^+}$ to be satisfied. In order to obtain further relations it is necessary to solve (3.16).

We can obtain some useful relations for the region $\omega \rightarrow 1$ by remarking that the driving term dominates in this limit. We have already used this feature several times, and will do so again. Equation (3.16) then simplifies to the first term, and apart from $F^{K^+} = F^{\pi^+}$ (U-spin), the other particle ratios are given by Clebsch-Gordon coefficients for D-coupling,

$$\lim_{\omega \rightarrow 1} \frac{F^{K^0}}{F^{K^+}} = \frac{2}{5}$$

(3.17)

$$\lim_{\omega \rightarrow 1} F^{\eta}/F^{K^+} = \frac{3}{5}$$

One can even get a ratio $\eta'/K^+ = \frac{4}{5}$ in this limit, if the η' is pure SU_3 singlet but one uses the nonet d_{ijk} .

In dual or quark parton models the above relations are lower bounds (14,15,7).

IV. Multichannel Effects

1. We will now consider some modifications to the bare bones model. Our aim is to see what changes this introduces in the results of the preceding sections. We are principally interested in seeing what happens when we relax the assumption that the decaying hadron system keeps $J = 1$. For example, one could imagine that the system carries out a random walk in J as it decays. By virtue of the scaling property of the model, and the logarithmic multiplicity, the number of jumps on a Chew-Frautschi plot only grows as $\ln s$, and we expect that a random walk in J during the decay will lead to predominantly low J values. It seems worthwhile to simplify the problem by considering a decay chain in which all particles have even G -parity and the spin is replaced by some other label. For technical reasons which will become obvious, we also to restrict the problem to one with only two decaying states. We thus imagine that the initial state (which we shall call ρ) can radiate a $G = +$ "pion", $\rho \rightarrow \rho\pi$, make a transition $\rho \rightarrow A\pi$ (or the reverse), or that the particle "A" can radiate, $A \rightarrow A\pi$. The vertices are characterized by couplings $\lambda_{1,\mu}$ and λ_2 , together with associated vertices K_1 , K_μ and K_2 as in Sect. II.

We do not think it necessary to include the spin explicitly but we might mention that if our $G = +$ "pion" were pseudoscalar, the ρ had $J = 1$ and the A $J = 2$, then all the vertices would involve the same type of spin factors, which can be explicitly removed from the problem. The extra kinematic factors coming from the spin of the A are included in the explicit form of $K_{\mu,2}$.

Hopefully this two component example can give us some insight into the features of chain emission models when multiple spin transitions are allowed.

2. If we now assume that all the vertices scale, just as in the case treated in Sect. II, we can directly write down the expression for the Mellin transformed ρ by summing over all possible configurations in Fig. 5,

$$\hat{\rho}(j) = \sum_{n=0}^{\infty} \hat{\rho}_n(j)$$

$$\hat{\rho}_n(j) = \sum_{r=0}^n \sum_{m=0}^{n-r} C_{mr}^n \frac{\lambda_1^{n-r-m}}{(n-r-m)!} \frac{\lambda_2^m}{m!} \frac{\lambda_2^r}{r!} (K_1(j))^{n-r-n} \times \quad (4.1)$$

$$\times (K_\mu(j))^m (K_2(j))^r \hat{\rho}_0(j)$$

where K here is just that introduced in Sec. II, with λ replaced by $\lambda_1, \lambda_2, \mu$. The cross section for production of $N = n+n_0$ pions is given in terms of the transform of $\rho_n(j)$, which is a homogenous function of λ_1, λ_2 and μ of degree n . The combinatoric problem to be solved lies in the calculation of the C_{mr}^n . Once this is done, we can get $\langle n \rangle$ and $\langle n^2 \rangle$, from the expressions ($\rho \equiv \rho(s, \lambda_1, \lambda_2, \mu)$)

$$\langle n \rangle \rho = \left(\lambda_1 \frac{\partial}{\partial \lambda_1} + \lambda_2 \frac{\partial}{\partial \lambda_2} + \mu \frac{\partial}{\partial \mu} \right) \rho \quad (4.2)$$

$$\langle n^2 \rangle \rho = \left(\lambda_1 \frac{\partial}{\partial \lambda_1} + \lambda_2 \frac{\partial}{\partial \lambda_2} + \mu \frac{\partial}{\partial \mu} \right)^2 \rho$$

just as we did in Sect. II for the less complicated case treated there.

3. The calculation of C_{mr}^n can be carried out by constructing the generating function of the problem (16). To do this, we need to keep two rules in mind: the vertices λ_1 and λ_2 are not allowed to be adjacent, and there can only be an even number of μ -vertices separating two identical sets of λ_1 or λ_2 vertices. The factors taking account of the identity of all the λ_1 vertices, etc., have already been included in (4.1).

Constructing the generating function requires some patience. It turns out to be

$$G(\lambda_1 \lambda_2 \mu) = \frac{1}{(1-\lambda_1)(1-\mu)} \frac{1 + [1]}{(1 - [1][2])}$$

$$[1] = \frac{\mu}{1-\mu^2} \frac{\lambda_2}{1-\lambda_2} + \frac{\mu^2}{1-\mu^2} \frac{\lambda_1}{1-\lambda_1} \quad (4.3)$$

$$[2] = \frac{\mu}{1-\mu^2} \frac{\lambda_1}{1-\lambda_1} + \frac{\mu^2}{1-\mu^2} \frac{\lambda_2}{1-\lambda_2}$$

C_{mr}^n is now obtained by differentiation

$$\begin{aligned}
C_{mr}^n &= \frac{\partial^{n-r-m}}{\partial \lambda_1^{n-r-m}} \frac{\partial^m}{\partial \mu^m} \frac{\partial^r}{\partial \lambda_2^r} G(\lambda_1 \lambda_2 \mu) \Big|_{\lambda_1 = \lambda_2 = \mu = 0} \\
&= G^{(n-m-r, m, r)}(0, 0, 0)
\end{aligned} \tag{4.4}$$

We can now go back to (4.1), writing it as a Taylor series,

$$\begin{aligned}
\hat{\rho}(j) &= \hat{\rho}_0(j) \sum_{n=0}^{\infty} \sum_{m=0}^n \sum_{r=0}^{n-m} \frac{(\lambda_1 K_1)^{n-m-r}}{(n-m-r)!} \times \\
&\times \frac{(\mu K_\mu)^m}{m!} \frac{(\lambda_2 K_2)^r}{r!} G^{(n-m-r, m, r)}(0, 0, 0)
\end{aligned} \tag{4.5}$$

from which we see at once that

$$\hat{\rho}(j) = \hat{\rho}_0(j) G(\lambda_1 K_1, \lambda_2 K_2, \mu K_\mu) \tag{4.6}$$

4. The asymptotic behavior of $\rho(s)$ is determined by the leading poles of $\hat{\rho}(j)$, which are in turn given by the zeros of the denominator $g^{-1}(\lambda_1 K_1, \lambda_2 K_2, \lambda K_\mu)$,

$$g^{-1} = 1 - [1] [2] \tag{4.7}$$

with [1] and [2] as in (4.3). Now we want to introduce a simplification by choosing $K_1 = K_2 = K_\mu = K$. Then the leading singularities are given by $(\alpha = \alpha(\lambda))$,

$$g^{-1}(\lambda_1 K(\alpha), \lambda_2 K(\alpha), \mu K(\alpha)) = 0 \tag{4.8}$$

where

$$1 - \lambda K(\alpha) = 0 \tag{4.9}$$

determines $\alpha(\lambda)$ if λ is given by a solution of (4.8) with K replaced by $1/\lambda$.

From (4.3), (4.8) and (4.9), it is a simple matter to see that λ is a solution of the eighth order polynomial

$$\begin{aligned}
 P(\lambda) = & (\lambda^2 - \mu^2) [(\lambda - \lambda_0)^2 - \delta^2] \\
 & - \mu^2 [\lambda(\lambda_0 - \delta)(\lambda - \lambda_0 - \delta) + \mu(\lambda_0 + \delta)(\lambda - \lambda_0 + \delta)] \times \\
 & \times [\lambda(\lambda_0 + \delta)(\lambda - \lambda_0 + \delta) + \mu(\lambda_0 - \delta)(\lambda - \lambda_0 - \delta)]
 \end{aligned} \tag{4.10}$$

where $2\lambda_0 = \lambda_1 + \lambda_2$, and $2\delta = \lambda_1 - \lambda_2$. We now choose $\lambda_2 < \lambda_1$ and note that $P(\lambda_2) < 0$, $P(\lambda_0) > 0$, $P(\lambda_1) < 0$. Thus, in the interval between λ_2 and λ_1 we have two solutions (Fig. 6) which we denote by λ_{\pm} , $\lambda_2 < \lambda_- < \lambda_0 < \lambda_+ < \lambda_1$.

From the preceding, we see that the presence of two channels leads to a classic split-level problem. We will refer to α_+ and α_- as the "up" and "down" solutions. Then $\rho(s)$ is given by

$$\rho(s, \lambda_1, \lambda_2, \mu) = \frac{1}{2} (\rho_+ + \rho_-) \tag{4.11}$$

where $\rho_{\pm} = C_{\pm} s^{\alpha_{\pm}}$ with $\lambda_{\pm} K(\alpha_{\pm}) = 1$. This solution has the expected properties: (i) as $\lambda_1, \lambda_2 \rightarrow \lambda(\delta \rightarrow 0)$ we have $\lambda_{\pm} \rightarrow \lambda$ and $C_{\pm} \rightarrow C$; (ii) as $\mu \rightarrow 0$, $\lambda_{\pm} \rightarrow \lambda_1$ and $C_{\pm} \rightarrow C$. We will not need the C_{\pm} in the following discussion.

5. From (4.2), the asymptotic mean multiplicity can be calculated to be

$$\langle n \rangle = \frac{1}{2} (n_+ + n_-) - \frac{1}{2} (n_+ - n_-) (1 - s^{-(\alpha_+ - \alpha_-)}) \tag{4.12}$$

where $n_{\pm} = (\lambda \frac{\partial \alpha}{\partial \lambda})_{\pm} \ln s$. From this we see that the multiplicity increases more slowly than $\ln s$ at finite energies. This is because the second term above is negative. We can see this by noting that $\lambda \partial \alpha / \partial \lambda$ increases monotonically (see Sec. II) in λ , leading to $n_+ > n_-$. Physically, there are two modes contributing to the total multiplicity, which is depressed at non-asymptotic energies by the presence of the second component n_- . Asymptotically this component dies away and $\langle n \rangle \rightarrow \langle n_+ \rangle$.

The most interesting effect of the coupled channels lies in the dispersion or the behavior of $f_2 = \langle n(n-1) \rangle - \langle n \rangle^2$. We have, parallel to the result in Sec. III,

$$\begin{aligned}
& \langle n^2 \rangle - \langle n \rangle^2 \\
&= \langle n \rangle + \left(\lambda^2 \frac{\partial^2 \alpha}{\partial \lambda^2} \right)_{\text{Av}} \ln s + \frac{\rho_+ \rho_-}{4 \rho} (n_+ - n_-)^2
\end{aligned} \tag{4.13}$$

where

$$\left(\lambda^2 \frac{\partial^2 \alpha}{\partial \lambda^2} \right)_{\text{Av}} = \frac{1}{2} \left[\left(\lambda^2 \frac{\partial^2 \alpha}{\partial \lambda^2} \right)_{\lambda=\lambda_+} + \left(\lambda^2 \frac{\partial^2 \alpha}{\partial \lambda^2} \right)_{\lambda=\lambda_-} \right]$$

We see that the presence of two channels tends to broaden the distribution at non-asymptotic energies. This is again what we might have expected: there are two components at different n_{\pm} and this makes the overall distribution in n broader than for each component alone. Of course at asymptotic energies

$$\begin{aligned}
\rho &= \rho_+ = \frac{1}{2} C_+ s^{\alpha_+} \\
\langle n \rangle &= n_+ = \left(\lambda \frac{\partial \alpha}{\partial \lambda} \right)_{\lambda=\lambda_+} \\
f_2 &= \left(\lambda^2 \frac{\partial^2 \alpha}{\partial \lambda^2} \right)_{\lambda=\lambda_+} \ln s
\end{aligned} \tag{4.14}$$

Clearly, the inclusion of a second component will modify some of the conclusions in Sects. II-III so long as the energies are not "truly" asymptotic. This depends, of course, on dynamical details (the exact values of α_+ and α_-). Before, we had leading $s^{\alpha(\lambda)}$ dependence for $\rho(s)$ and now it is split, as in (4.11). Now we can have distributions much broader than those in the single component case, clearly, adding more components would accentuate this. However, we expect the qualitative features discussed in Sect. II-III to be restored at sufficiently high energies.

V. Two-Particle Inclusive Distributions

1. We shall now turn to the two particle inclusive process $e^+e^- \rightarrow \pi^\alpha(P_1) + \pi^\beta(P_2) + H$ for which we can obtain some useful lessons from the spin and isospin dependence of the bare bones model. The kinematics of the twice inclusive process has been treated elsewhere (17,18). We shall refer to Ref.(18) for the necessary details, and simply cite the material we require. The dynamics is contained in the hadronic tensor

$$\begin{aligned}
 W_{\mu\nu}^{\alpha\beta}(P_1, P_2, Q) &= \frac{1}{4\pi} \sum_H \delta(Q - P_1 - P_2 - P_H) \times \\
 \langle 0 | J_\mu(0) | \pi^\alpha(P_1), \pi^\beta(P_2), H \rangle &\times \\
 \times \langle \pi^\alpha(P_1), \pi^\beta(P_2), H | J_\nu(0) | 0 \rangle &
 \end{aligned} \tag{5.1}$$

We shall need the decomposition of this into invariant amplitudes, which reads

$$\begin{aligned}
 W_{\mu\nu}^{\alpha\beta}(P_1, P_2, Q) &= \sum_{i=1}^5 \Gamma_{\mu\nu}^i W_i^{\alpha\beta}(Q^2, \omega_1, \omega_2, \eta_{12}) \\
 \Gamma_1^{\mu\nu} &= g^{\mu\nu} - Q^\mu Q^\nu / Q^2 \\
 \Gamma_2^{\mu\nu} &= \hat{P}_1^\mu \hat{P}_1^\nu \\
 \Gamma_3^{\mu\nu} &= \hat{P}_2^\mu \hat{P}_2^\nu \\
 \Gamma_4^{\mu\nu} &= \frac{1}{2} [\hat{P}_1^\mu \hat{P}_2^\nu + \hat{P}_1^\nu \hat{P}_2^\mu] \\
 \Gamma_5^{\mu\nu} &= \frac{i}{2} [\hat{P}_1^\mu \hat{P}_2^\nu - \hat{P}_1^\nu \hat{P}_2^\mu] \\
 \hat{P}_i^\mu &= P_2^\mu - (P \cdot Q) Q^\mu / Q^2
 \end{aligned} \tag{5.2}$$

We shall not need Γ_5 ; it is only measurable when longitudinally polarized e^+e^- beams are available. The invariant functions W_i depend on the kinematic invariants

$$\omega_1 = 2 P_1 \cdot Q/Q^2, \quad \omega_2 = 2 P_2 \cdot Q/Q^2$$

(5.3)

$$\begin{aligned} \eta_{12} &= (P_1 + P_2)^2/Q^2 \\ &= \omega_1 \omega_2 - \sqrt{\omega_1^2 - \frac{4m^2}{Q^2}} \sqrt{\omega_2^2 - \frac{4m^2}{Q^2}} \cos\theta_{12} \end{aligned}$$

or equivalently using the missing mass $M_x^2 = (1 - \omega_1 - \omega_2 + \eta_{12}) s$.

2. A complete discussion of this process is beyond our aims. We shall restrict the discussion to the case where one hadron (p_1 say) has $\omega_1 \sim 1$. Then we consider the dependence on ω_2 , $\cos\theta_{12}$, the angular variables, and isospin. This will demonstrate the usefulness of studying this kinematic region.

As an example, we might mention that already in the single particle inclusive case near $\omega \sim 1$, one can obtain information on the normality ($n = P(-)^J$ where P is the parity) of the system recoiling against the hadron with $\omega \sim 1$. This is the limit where one has two body $\pi + X$ form factors, and one can see from the parity rules of Ref. (19) that a system X of even normality cannot have a $\sin^2\theta$ component in the single particle distribution; a system of odd normality can. We shall see that a similar situation also occurs here for the two particle inclusive reaction (Fig. 7a) where we measure the angular dependence of P_2 with respect to P_1 as axis. This is analogous to what occurs in inclusive electroproduction $e + H \rightarrow e' + H' + X$ in the current fragmentation region, where definite normality in the Reggeon channel (Fig. 7b) has implications for the helicity amplitudes of the process and thus also for the angular dependence (azimuthal terms like those in Equ.(5.7) below. (20,21)

As to isospin, we can compare isospin (charge) correlations between one particle of definite charge at $\omega_1 \sim 1$ and another of the same or different charge as a function of ω_2 .

In all of this we shall stay with the bare bones model, where the hadron system keeps $J = 1$ and we have π emission with alternating isospins along the chain.

3. We concentrate now on $\omega_1 \sim 1$ because of the vast simplification it brings: only the first term in Fig. 4 is relevant, the others being suppressed by powers of $1 - \omega_1$ (II). We have already remarked on this in the single particle inclusive case. Here it means that we can forget many of the complications of the two-particle inclusive process. We have a factorization property from Fig.4: for $\omega_1 \sim 1$, the ω_2 distribution is given entirely in terms of structure functions for the single particle inclusive reaction with a current of different isospin from that of the photon. For the moment we shall suppress the isospin, writing

$$W_{\mu\nu}^2(P_1, P_2, Q) = |F(s, (1-\omega_1)s)|^2 \epsilon_{\mu\alpha\beta\gamma} \epsilon_{\nu\alpha'\beta'\gamma'} \times \quad (5.4)$$

$$\times Q^\alpha P_1^\beta Q^{\alpha'} P_1^{\beta'} W^{\gamma\gamma'}(P_2, Q-P_1)$$

where $F(s, (1-\omega_1)s)$ is the invariant vertex and

$$W^{\mu\nu}(P_2, Q') = (g^{\mu\nu} - Q^\mu Q^\nu / Q^2) W_1(Q'^2, \omega_2) \quad (5.5)$$

$$+ \hat{P}_2^\mu \hat{P}_2^\nu W_2(Q'^2, \omega_2)$$

The results are most transparent if we write them in terms of helicity structure functions defined in the lab system with z-axis along \underline{p}_1 and x-axis lying in the plane defined by and the e^+e^- collision axis. Then we define

$$H_{\lambda\lambda'} = \epsilon_\lambda^\mu \epsilon_{\lambda'}^\nu {}^* W_{\mu\nu}^{(2)} \quad (5.6)$$

where

$$\epsilon_\pm^\mu = \mp 1/\sqrt{2} (0, 1, \pm i, 0)$$

$$\epsilon_0^\mu = (0, 0, 0, 1)$$

Now take the angle of \underline{p}_1 with respect to the beam axis (the e^- momentum, say) to be θ and take the vector \underline{p}_2 to lie in a plane defined by \underline{p}_2 and \underline{p}_1 and rotated by an angle ϕ with respect to the x-z plane. Then the cross section reads⁽¹⁸⁾

$$\begin{aligned}
\frac{d^6\sigma}{dv^3 d^3R} &= \frac{3}{4} (1+\cos^2\theta) \frac{d^3\sigma_U}{dv^3} \\
&+ \frac{3}{4} \sin^2\theta \frac{d^3\sigma_L}{dv^3} + \frac{3}{4} \sin^2\theta \cos^2\phi \frac{d^3\sigma_T}{dv^3} \\
&- \frac{3}{2\sqrt{2}} \sin^2\theta \cos\phi \frac{d^3\sigma_I}{dv^3}
\end{aligned} \tag{5.7}$$

where

$$\frac{d^3\sigma}{dv^3} = \frac{32\pi \alpha^2 p_1 p_2}{3 s^2} H_\alpha \quad ; \quad \alpha = U, L, T, I$$

and

$$\begin{aligned}
H_U &= \frac{1}{2} (H_{++} + H_{--}) \\
H_L &= H_{00} \\
H_T &= H_{+-} \\
H_I &= \text{Re } H_{+0}
\end{aligned} \tag{5.8}$$

$$dv^3 = d\omega_1 d\omega_2 d \cos\theta_{12} \quad ; \quad d^3R = d \cos\theta d\phi \tag{5.9}$$

Now we simply calculate from 5.4, obtaining

$$\begin{aligned}
H_{++} &= |F(s, (1-\omega_1)s)|^2 s p_1^2 (W_1 + \frac{1}{2} p_{2T}^2 W_2) \\
H_{+-} &= |F(s, (1-\omega_1)s)|^2 s p_1^2 (\frac{1}{2} p_{2T}^2 W_2) \\
H_{+0} &= 0 \\
H_{00} &= 0
\end{aligned} \tag{5.10}$$

where $W_i = W_i((1-\omega_1)s, \omega_2)$, with ω_2 the scaling variable for the system recoiling against particle 1 (we already used this in Sect. II). It is given by

$$\omega_2 = \omega_2 \frac{1 - \frac{1}{2} \omega_1 (1 - \cos \theta_{12})}{1 - \omega_1} \quad (5.11)$$

4. Now we can see that there is a great simplification in (5.7), most of the terms being zero,

$$\frac{d^6 \sigma}{d^3 v dR^3} \underset{\omega_1 \rightarrow 1}{\sim} \frac{3}{4} (1 + \cos^2 \theta) \frac{d^3 \sigma_v}{dv^3} + \frac{3}{4} \sin^2 \theta \cos 2\phi \frac{d^3 \sigma_T}{dv^3} \quad (5.12)$$

Additionally, we can note that $P_{2T} = \frac{1}{2} \omega_2 \sqrt{s} \sin \theta_{12}$ so as to see that for $\omega_2 \rightarrow 0$, $H_{+-} \rightarrow 0$ also. Equation (5.12) is a consequence of the normality structure of the initial pion emission vertex in Fig. 7a. It depends only on the fact that the recoiling mesonic system has even normality. We can check this for an $n = +$ system of spin J (polarization vector $e^{\alpha_1 \dots \alpha_J}$) which has a vertex proportional to

$$\varepsilon_{\mu\alpha_1\sigma\tau} Q^\sigma p_1^\tau p_{1\alpha_1} \dots p_{1\alpha_J} e^{\alpha_1 \dots \alpha_J} \quad (5.13)$$

which leads to the same structure as the above. This result changes, however, when we change the normality of the vertex. The $n = -$ vertex which gives a $\sin^2 \theta$ component to the single particle inclusive distribution is

$$(Q \cdot Q' g_{\mu\alpha_1} - Q'_\mu Q_{\alpha_1}) p_{1\alpha_2} \dots p_{1\alpha_J} e^{\alpha_1 \dots \alpha_J} \quad (5.14)$$

and we can verify by a straightforward calculation that H_{++} , H_{+-} , and H_{+0} are proportional to $(1 - \omega_1)^2$, while H_{00} survives as $\omega_1 \rightarrow 1$,

$$H_{00} \gg H_{++}, |H_{+-}|, |H_{+0}| \quad (5.15)$$

5. We see from the preceding that two particle inclusive distributions can be used to study the spin structure of the vertices in chain emission models. Extending this observation, we can obtain a test of the general idea of such models as we have formulated them. This class of models rest on the assumption that the system recoiling against a pion has low spin ($J = 1$ in the bare bones model). For the case $\omega_1 \rightarrow 1$ it is useful to carry out a Lorentz transformation

to the rest frame of the recoil system and then consider the angular distribution of particle 2 in this frame (the z-axis is still parallel to \underline{p}_1). The azimuthal dependence is contained already in (5.7) and the discussion above. If we define θ^* to be the angle between \underline{p}_2' and the z-axis in the rest frame of the recoil system, then clearly the polar angle dependence in this frame cannot be of very high order in $\cos\theta^*$, since we have assumed that the decaying system has small J (again, $J = 1$ in the bare bones version). It is evident that sharply peaked distributions (along the z-axis) would not be consistent with any model where the intermediate J is restricted.

A second remark follows directly on this one. Since for fixed ω_1 and $s \rightarrow \infty$ the mass of the recoil system grows proportional to $[(1-\omega_1)s]^{1/2}$, the limitation of J and the scaling property in ω_2 for the decay of this recoil system lead unavoidably to the conclusion that the model cannot have bounded momenta transverse to \underline{p}_1 . At low energies there might appear to be a cutoff in transverse momentum, because the rapidly falling ω_2 distributions (they must vanish for $\omega_2 \rightarrow 1$) may be expected to lead to falling distributions transverse to \underline{p}_1 , as inspection of (5.11) will show. Asymptotically, however, the mean p_T perpendicular to \underline{p}_1 must grow asymptotically proportional to $(1-\omega_1)^{1/2} \sqrt{s}$. This depends critically on our assumption that the spin of the cascading hadron system remains small, and is a test of that feature of the model. This is quite unlike the situation in parton models, where p_T is bounded and in the rest frame of the system recoiling against \underline{p}_1 there must therefore appear a marked peaking of the distribution of \underline{p}_2 parallel and antiparallel to \underline{p}_1 . Moreover we expect that for a rapid p_T cutoff the azimuthal dependences in (5.7) will all vanish at large s (18) (see, however, Ref. 22). Physically, the azimuthal dependences in chain emission models (e.g. $H_{+-} \neq 0$ for a pure $n = +$ recoiling system) are due to the fact that the recoil system has $J \geq 1$ and is transversely polarized. The azimuthal dependence is then a reflection of the angular distribution of the decay of this polarized system. In the spin one half parton model, such asymmetries vanish because of the rapid p_T cutoff.

The preceding remarks would be altered if we allowed the recoiling hadron system in the model to have large J ; the distributions would then become peaked from the decay distribution of the high- J system. We wish to indicate briefly how this could occur, and point out that such a phenomenon can be put in a general context, a timelike analogue of the Mueller-Regge discussion of the inclusive

distributions $\gamma_{\nu} + h \rightarrow h' + X$ (20). In that case one starts with a t-channel six point function and carries out a generalized Sommerfeld-Watson transformation and introducing a helicity-pole limit. We wish to take over the apparatus of Ref. (20) to the case at hand where Q^2 is timelike and so are two of the three Reggeon t-values (i.e. we assume that one can cross from one region to the other, preserving at least the functional form of the multiregge expansion). In this way we obtain for the helicity structure functions the following expression (understood to be a local average in $(1-\omega_1)s$):

$$\begin{aligned}
 H_{\lambda\lambda'} &= \beta_{\lambda}^* (s, (1-\omega_1)s) \beta_{\lambda'} (s, (1-\omega_1)s) \cdot \\
 &\cdot \left[\frac{1-\omega_2}{1-\omega_1-\omega_2 + \frac{1}{2} \omega_1 \omega_2 (1-\cos\theta_{12})} \right]^{2\alpha((1-\omega_1)s)} \times \\
 &\times F(\alpha, -\alpha, M_X^2, (1-\omega_1)s, (1-\omega_1)s, t_3 = 0)
 \end{aligned}
 \tag{5.16}$$

The expansion is a helicity-pole limit of Figs. (8a), (8b); $t_1 = t_2 = (1-\omega_1)s$. F is a reggeon inclusive decay distribution and the quantity in square brackets is the asymptotic variable (a t-channel azimuthal angle - see Ref. (20)). If we now assume that the residue scales, i.e.

$$\beta(s, (1-\omega_1)s) \rightarrow s^{\gamma} \bar{\beta}((1-\omega_1)s)$$

as $s \rightarrow \infty$, ω_1 fixed, and further that $\alpha(t)$ is linear in t, we see that the $\cos\theta_{12}$ distributions entering (5.16) are strongly peaked forward and backward, when

$$\frac{1-\omega_2}{1-\omega_1-\omega_2 + \frac{1}{2} \omega_1 \omega_2 (1-\cos\theta_{12})} \gg 1$$

Expressed in terms of $P_{\perp} = p_2 \sin\theta_{12}$, we find that as $s \rightarrow \infty$, $1 \gg (1-\omega_1)$, $(1-\omega_1-\omega_2) > 0$, the transverse momentum distributions are contained in a factor

$$\exp \left\{ -2\alpha \left[\frac{\omega_1 (1-\omega_1)}{1-\omega_1-\omega_2} p_{\perp}^2 \right] \right\}$$

provided $p_{\perp}^2 < (1-\omega_1-\omega_2)s$.

The model discussed in this section, either Reggeized or in its simple fixed spin version may be the relevant mechanism for this kinematic region, in dependent of the main details of the cascade mechanism, since the integral or iterative term vanishes as $\omega_1 \rightarrow 1$ mainly for kinematic reasons. It is therefore also worthwhile to consider the role played by isospin, which we discuss next, and is independent of the spin issue.

6. When we consider the isospin dependence of the bare bones model, we see that it predicts marked charge correlations for $\omega_1 \rightarrow 1$. Let us first consider the isovector component of the photon. By referring to Fig. 9a one can readily see that

$$(1) \quad W_{I=1}^{\pm\beta} = 0 \quad \text{and} \quad W_{I=1}^{0\beta} \quad \text{is non-zero to leading order in } 1-\omega_1, \text{ and is independent of } \beta (\alpha, \beta = +, -, 0).$$

Similarly, referring to Fig. 9b, one has for the isoscalar photon case

$$(2) \quad W_{I=0}^{\alpha\beta} \sim W_{I=0}^{\alpha, -\alpha} \delta_{\beta, -\alpha} \quad \text{for } \omega_2 \sim 1 \text{ or } \omega_2 \sim 1-\omega_1 \quad (\cos\theta_{12} \sim 1)$$

Putting this together with an isoscalar/isovector ratio of 1/3 we find for the region $\omega_1 \sim 1$:

$$(3) \quad W^{0\beta} \gg W^{\pm\beta} \quad \text{for all } \omega_2 \text{ and } \beta = +, -, 0.$$

$$(4) \quad W^{00} > W^{0+} \gg W^{+-} \quad \text{for } \omega_2 \sim 1 \text{ or } 1 - \omega_1 \quad (\cos\theta_{12} \sim 1)$$

$$(5) \quad W^{++} = W^{--} \sim W^{\pm 0} \sim 0 \quad \text{for } \omega_2 \sim 1 \text{ or } 1 - \omega_1 \quad (\cos\theta_{12} \sim 1).$$

(3)-(5) imply marked differences in $d\sigma/d\omega_1 d\omega_2$ for the different charge configurations. We illustrate this schematically in Figs. 10a,b,c, where we compare $\alpha, \beta = (0,+), (+,-)$ and $(+,+)$, plotted as a function of the variable $\tilde{\omega}_2 = \text{sign}(\cos\theta)\omega_2$.

We have considered the bare bones model here because it shows in a clear way how charge correlations can tell us about the isospin structure of the chain. The same arguments can be repeated for other chains of different isospin structure. We reiterate the remark in Sec.III that the above reflect the octet character of the recoiling system. By contrast, one cannot have such dramatic effects in the parton model where the fragmentating states are

triplets (quarks) /7/, /23/, /24/. Of course, statements like $W^{++} \ll W^{+-}$ as $\omega_1, \omega_2 \rightarrow 1$ is a reflection of the suppression of exotic states in the missing mass and is presumably independent of the model.

VI. Non-Linear Effects

So far we have discussed the linear chain model and its variations. We remarked in the introduction that such a model can be understood as an extension of the low energy production of states like $\pi\omega$, allowing the ω to go off shell as Q^2 increases. A similar fate could occur to low energy processes like $e^+e^- \rightarrow \rho^+\rho^-$. The ρ mesons being allowed off shell as the CM energy increases. This branching into two off-shell states introduces nonlinearities into the original model. Besides mentioning this possibility we should note that the entire model would look suspicious if $\alpha(\lambda)$ could become arbitrarily large; if we were not dealing with a two-point function, one would suspect the model of being in some sense non-unitary for large $\alpha(\lambda)$.

Some time ago, Polyakov⁽²⁵⁾ showed that one could rewrite the discontinuity equation for the propagator in a form similar to unitarity equations. We shall show here that the inclusion of nonlinear effects via a somewhat similar expansion (but with the linear chain as driving term) leads to a constraint on the value of $\alpha(\lambda)$. For small enough $\alpha(\lambda)$ the nonlinear effects are of little importance at asymptotic energies. Therefore there are conditions under which the linear chain model is stable against the introduction of such branching effects.

The equations, including nonlinear terms, are diagrammed in Fig.(11). Note that the interference terms shown in Fig.(11a) have to be explicitly included, as they would not appear on iteration of the remainder. A new branching vertex appears, $V(Q^2, \sigma_1^2, \sigma_2^2)$. This represents the amplitude for the initial state to branch into two similar states of masses $\sqrt{\sigma_1^2}$ and $\sqrt{\sigma_2^2}$. For the two-propagator term shown in Fig.(11b), we have

$$\begin{aligned}
 (6.1) \quad \rho^{(2)}(s) &= \int \frac{d^4 Q_1}{(2\pi)^4} |V(Q^2, Q_1^2, (Q-Q_1)^2)|^2 \int d\sigma_1^2 \rho(\sigma_1^2) 2\pi \delta^+(Q_1^2 - \sigma_1^2) \\
 &\quad \times \int d\sigma_2^2 \rho(\sigma_2^2) 2\pi \delta^+((Q-Q_1)^2 - \sigma_2^2) \\
 &= \int d\sigma_1^2 d\sigma_2^2 \rho(\sigma_1^2) \rho(\sigma_2^2) |V(Q^2, \sigma_1^2, \sigma_2^2)|^2 \Pi_2(Q^2, \sigma_1^2, \sigma_2^2)
 \end{aligned}$$

$\Pi_2(Q^1, \sigma_1^2, \sigma_2^2) = \Delta(Q^1, \sigma_1^2, \sigma_2^2)/4\pi s$ is the two body phase space factor, where $\Delta(Q^2, \sigma_1^2, \sigma_2^2) = \theta(\lambda) \lambda^{1/2}(Q^2, \sigma_1^2, \sigma_2^2)$, λ being the usual triangle function.

Introducing Mellin transforms as in Sec.II and writing $\sigma_i^2 = \eta_i s$ we can rewrite (6.1) as

$$(6.2) \quad \rho^{(2)}(s) = \frac{1}{4\pi} \int \frac{dj_1}{2\pi i} \frac{dj_2}{2\pi i} \hat{\rho}_o(j_1) \hat{\rho}_q(j_2) s^{j_1+j_2} \\ \times \int d\eta_1 d\eta_2 \Delta(1, \eta_1, \eta_2) \eta_1^{j_1} \eta_2^{j_2} s^2 |V(s, \eta_1 s, \eta_2 s)|^2 .$$

The contours run from $-i\infty$ to $+i\infty$ to the right of all singularities.

We shall study the case $\eta_1, \eta_2 > 0$, in conformance with our practice of assuming dominance of the off-shell region in the equations. We further assume again a scaling law (μ is a convenient scale factor)

$$(6.3) \quad s^2 |V|^2 \rightarrow \mu s^{-\delta} |\phi_\delta(\eta_1, \eta_2)|^2$$

as $s \rightarrow \infty$. Now we take the Mellin transform of $\rho^{(2)}(s)$ and find

$$(6.4) \quad \hat{\rho}^{(2)}(j) = \left(\frac{\mu^2}{4\pi^2} \right) \int \frac{dj_1}{2\pi i} \frac{dj_2}{2\pi i} \hat{\rho}(j_1) \hat{\rho}(j_2) \frac{\phi_\delta^{(2)}(j_1, j_2)}{(j-j_1-j_2+\delta)}$$

where

$$\phi_\delta^{(2)}(j_1, j_2) = \int d\eta_1 d\eta_2 \Delta(1, \eta_1, \eta_2) \eta_1^{j_1} \eta_2^{j_2} |\phi_\delta|^2 .$$

The corresponding analysis of the interference term Fig.(11c) is more involved. Written out in the same way as $\rho^{(2)}$,

$$(6.5) \quad \rho^{(3)}(s) = \int d\sigma_1^2 d\sigma_2^2 d\sigma_3^2 \rho(\sigma_1^2) \rho(\sigma_2^2) \rho(\sigma_3^2) \times \\ \times \int \frac{d^4 Q_1}{(2\pi)^4} \frac{d^4 Q_2}{(2\pi)^4} 2\pi \delta^+(Q_1^2 - \sigma_1^2) 2\pi \delta^+(Q_2^2 - \sigma_2^2) 2\pi \delta(Q_3^2 - \sigma_3^2) \times \\ \times V^+(s, (Q_2+Q_3)^2, \sigma_1^2) V^+((Q_2+Q_3)^2, \sigma_2^2, \sigma_3^2) \\ \times V((Q_1+Q_2)^2, \sigma_1^2, \sigma_2^2) V(s, (Q_1+Q_2)^2, \sigma_3^2) .$$

The reduction of the three-body phase space integral involves some algebra; we only state the result.⁽²⁶⁾ Introducing the scaled variables ($Q^2 = s$)

$$\sigma_i^2 = \eta_i s \quad (Q-Q_i)^2 = (1 - \rho_i)s$$

and the cosine of the angle between the momenta of the "legs" 1 and 3

$$Z = \cos\theta_{13} = 2(\rho_1^2 - 4\eta_1^2)^{1/2}(\rho_3^2 - 4\eta_3^2)^{1/2} \times \\ \times \left\{ \eta_1 + \eta_3 + \frac{1}{2} \rho_1 \rho_3 - 1 + \rho_1 + \rho_3 + \eta_2 \right\}$$

we have for the Mellin transform of $\rho^{(3)}(s)$

$$(6.6) \quad \rho^{(3)}(j) = \frac{\pi}{16} \left(\frac{\mu^2}{4\pi^2} \right)^2 \int \frac{dj_1}{2\pi i} \frac{dj_2}{2\pi i} \frac{dj_3}{2\pi i} \hat{\rho}(j_1) \hat{\rho}(j_2) \hat{\rho}(j_3) \times \\ \times \frac{\phi_\delta^{(3)}(j_1, j_2, j_3)}{j - j_1 - j_2 - j_3 + 2\delta}$$

where, allowing for the other interference term,

$$\phi_\delta^{(3)} = \text{Re} \left\{ \int d\rho_1 d\rho_2 d\eta_1 d\eta_2 d\eta_3 \theta(\rho_1^2 - 4\eta_1^2) \cdot \right. \\ \cdot \theta(\rho_3^2 - 4\eta_3^2) \theta(1 - |Z|) \frac{j_1}{\eta_1} \frac{j_2}{\eta_2} \frac{j_3}{\eta_3} \cdot \\ \cdot \phi_\delta((1-\rho_1), \eta_1) \phi_\delta(\eta_2/(1-\rho_1), \eta_3/(1-\rho_1)) \cdot \\ \left. \cdot \phi_\delta(\eta_1/(1-\rho_3), \eta_2/(1-\rho_3)) \phi_\delta((1-\rho_3), \eta_3) \right\} \cdot$$

At this point it is appropriate to remark that we can treat a type of diagram not included in Figs.(11a-c) (i.e. Fig.(12d), where the propagator is replaced by a pion and μV by λF , the pion radiation vertex) by setting $\sigma_3^2 = m_\pi^2$. In the model without spin this leads to a kernel of the same general structure as (7) with $j_3 \rightarrow 0$ and $2\delta \rightarrow \delta$ in (6). This will lead to a singularity to the left of that in (6), and to a contribution which decreases faster asymptotically in s than the interference term of Fig.11c.

From this we see that the Mellin transformed integral equation - including even complicated interference terms - will have the form

$$(6.8) \quad \hat{\rho}(j) = \hat{\rho}_0(j) + \lambda K(j) \hat{\rho}(j) \\ + \sum_{N=2}^{\infty} \left(\frac{\mu^2}{4\pi^2} \right)^{N-1} \int \prod_{\kappa=1}^N \frac{dj_{\kappa}}{2\pi i} \hat{\rho}(j_{\kappa}) \frac{\Phi_{\delta}^{(N)}(j_1 \dots j_N)}{j-j_1^{-} \dots -j_N^{+} (N-1)}$$

We shall not attempt to solve this, but rather search for a condition under which the linear chain survives as the asymptotically dominant contribution to $\rho(s)$. An obvious precondition for this is that the sum in (8) make sense. To find the condition, we demand that $\hat{\rho}(j)$ have the same leading j plane pole as the linear chain itself (see Sec.II),

$$\hat{\rho}(j) = \frac{r(j)}{j^{-\alpha(\lambda)}} + \dots$$

where $r(j)$ is regular at $j = \alpha$, and $\alpha(\lambda)$ is given by $1 - \lambda K(\alpha) = 0$ picking up the contribution of the rightmost poles in the sum in (8), we see that the condition we desire is that the remaining pole in the summation not lead that at $j = \alpha(\lambda)$, so

$$(6.9) \quad N \alpha(\lambda) - (N-1)\delta < \alpha(\lambda)$$

i.e. $\alpha(\lambda) < \delta$. The singularities of the summation now lie to the left of $\alpha(\lambda)$, and the eigenvalue condition for the linear chain determines the asymptotic behavior. The presence of the non linear effects is felt through the existence of a non linear equation for $r(j)$ which can be read off from (6.8). If we assume that the singularities of (6.8) besides those at $j = \alpha$ are known, then the integral remaining after extraction of the poles at $j = \alpha$ in the sum can be absorbed into the driving term. Under these conditions the equation for $r(\alpha)$ simplifies to the point that we can argue that as $\alpha(\lambda) \rightarrow \delta$ the residue $r(\alpha) \rightarrow 0$ - i.e. the linear chain decouples. This is most readily seen when the interference terms vanish (i.e. $\Phi^{(N)} = 0$ $N \geq 3$). This is clear from the fact that the quadratic term in $r(\alpha)$ is multiplied by $(\alpha - \delta)^{-1}$; $\alpha \rightarrow \delta$ corresponds to a solution $r(\alpha) \rightarrow 0$. We have checked that the same occurs for a wide variety of Ansätze for $\Phi^{(N)}$. This indeed looks like a condition putting an upper limit on $\alpha(\lambda)$ - a kind of unitarity condition. If this is unchanged when including other singularities than those which can be included into the driving term, we expect that for

$\alpha(\lambda) > \delta$ the nonleading terms will become the dominant ones. Presumably the branching process will then become the only relevant mechanism.

For $\alpha(\lambda) < \delta$, the main emission process is that due to the linear chain. The non linear effects arise at the end of the radiation process when the hadron system no longer has asymptotic masses (i.e. in the driving term). The particles in question have low ω , so that we have identified one more mechanism which ruins Feynman scaling at small ω and nonasymptotic energies.

We close by considering some of the qualitative differences between a linear chain model and a model where the branching process dominates. For this purpose we introduce the rapidity of the produced hadron $0 \leq y = \ln \frac{E+p}{m} \leq \ln \frac{\sqrt{s}}{m} = Y$. The chain model has a plateau of constant height for $\sigma^{-1} d\sigma/dy$ as long as $y > 2$ and $Y - y \geq 2$. This plateau grows in length proportional to Y . At finite $y \leq 2$ $\sigma^{-1} d\sigma/dy$ can grow in height proportional to Y ; we discussed this anomaly in Sec.II. The region $Y - y \leq 2$ is where the structure function falls rapidly in x corresponding to the fragmentation region in hadronic reactions. We might mention that the behavior of $\sigma^{-1} d\sigma/dy$ is similar in the parton model, except that no anomaly occurs for $y \leq 2$. See Figs. (12a) and (12b). Branching models are quite different; they have been discussed by Polyakov,⁽²⁵⁾ and, in a different form, by Rittenberg and Orfanidis.⁽²⁷⁾ Under certain assumptions $\sigma^{-1} d\sigma/dy$ becomes proportional to a gaussian in y , the width growing as \sqrt{Y} . Neglecting the width, the distribution is centered at $\bar{y} \approx (1-\epsilon)Y$ where ϵ is given in terms of the multiplicity growth, $\langle n \rangle \propto (Q^2)^{\epsilon/2}$ (see Fig.12c). A power growth of n , $\epsilon > 0$, is typical for such models - independent of the precise form of $\sigma^{-1} d\sigma/dy$ - as is the conclusion that KNO scaling holds, $\sigma_n/\sigma = \langle n \rangle^{-1} \psi(n/\langle n \rangle)$. In the model of Ref.(27), the gaussian form holds provided $|y-\bar{y}|$ is not too large. In general, then, the area under $\sigma^{-1} d\sigma/dy$ increases as $e^{\epsilon Y}$ in such models.

All these statements hold for large Y . In the linear chain (or parton) models one needs $Y \gtrsim 5-6$ for the full structure to appear; for branching models, similarly large Y should be necessary as the number of "branches" per event (proportional to μ^N in Eq.(6.8)) is proportional to Y . Such large values of Y correspond to $\sqrt{s} \gtrsim 40-50$ GeV. At presently attainable values of $\sqrt{s} \sim 5-8$, $Y \sim 3-4$ and most models can probably be made to look like the data, which shows a hump in y of width ≈ 2 units.⁽²⁷⁾

At such low energies correlation measurements of the sort discussed in the preceding section may help to sort out the different physical mechanisms which might be responsible for e^+e^- annihilation.

VII. Conclusions

We wish to recapitulate briefly what we have learned. We have studied chain-emission (cascade) models for e^+e^- annihilation. Such models lead for a power law behavior for the e^+e^- total cross-sections, somewhat analogous to the multiperipheral model for hadronic total cross-section, however in the latter case the power law is restricted by unitarity. Although a forward unitarity condition restricting the power is absent in e^+e^- annihilation, a unitarizing mechanism can be constructed. This was discussed in Sec.VI. The chain models lead to Feynman scaling, except in the limit $\omega \rightarrow 0$, where it is broken in a well defined way. The multiplicity grows as $\ln s$, and an instructive feature of the models is that the coefficient of this logarithmic growth is not given simply by integrating the scaling function down to its lower limit. Since the model is solvable, it is possible to use the energy sum rule to study the approach of the cross section to its asymptotic limit, which is from below. These features have been discussed before (I,II), but we treat them here to emphasize their generality.

Since our main aim in this paper is pedagogical, we carried out much of the discussion for a simplified version of such models, in which the spin of the decaying hadron system is fixed at $J = 1$ while it emits pions, the isospin of the hadron system alternating $I = 0, 1$. We find that, although the ratio of neutral to charged pions approaches $1/2$ asymptotically, it only does this logarithmically in energy. More interesting, the alternating-isospin model offers an explicit example of how the ratio of neutral energy to charged energy (total) can deviate even at asymptotic energies from $1/2$. We conclude that if, in fact, the neutral pions carry off much more energy on the average than the charged ones then the isospin structure of the chain is strongly restricted. Further information on the isospin structure of the model can be gained from studying the mean number of neutral pions for a fixed number of charged pions. Much more informative, however, is the behavior of the "branching ratio" of a state of fixed pion number into n_0 neutral and n_c charged pions. This contains the isospin structure in a particularly clear form. We go on to mention briefly how one can incorporate SU_3 into the model.

An important question in chain-emission models is whether they can be generalized to include other states than appear in our simple example. We have demonstrated that this can be done in the case of SU_3 symmetry. A more important case is that in which the hadron system which decays by emitting pions has spins other than the $J = 1$ of the simple model. We can claim no complete solution; instead we have studied the problem in a simple example where there are two states (e.g. with $J = 1$ and 2) with transitions possible between them. This is a coupled channel problem, and we see that the features of the simple model with one state are recovered at very high energies. At lower energies there can appear corrections: number distributions can become broadened due to the presence of two components, and so on. Considerations of this sort may also become important if one wishes to drop the assumption of alternating isospins which we have been using for illustrative purposes.

We go on to study two-particle inclusive e^+e^- annihilation. Here the properties of the simple model show themselves most clearly. We study the particularly useful case where one hadron has large momentum $\omega_1 \approx 1$. Then we find that the mean momentum of the second particle transverse to the axis defined by the first should grow asymptotically like $[(1-\omega_1)^{1/2}\sqrt{s}]$, i.e. there is no transverse momentum cut off. However since the coefficient of the growth is small in the $\omega_1 \sim 1$ region, large transverse momenta will only be seen at very high energies]. The cross section for the second particle turns out to have an important dependence on the azimuthal angle about the direction of the first particle. This is unlike the situation in parton models with spin $1/2$ partons and a transverse momentum cutoff. In fact, these azimuthal dependences have, in chain-emission models, useful information on the normality of the system recoiling against one fast hadron. As a by-product of our discussion we note that it might be interesting to analyze the angular distribution of particle 2 in the rest frame of the system recoiling against the first (fast) particle. This can tell us about the spin of the recoil system and would check a fundamental assumption of the model: that the spin of the hadron system does not become large. We have also considered the possibility that the spin of the intermediate states are controlled by a regge trajectory in the time like region, in this case the spin grows slowly with s and a strong damping in p_{\perp}^2 emerges. In the latter situation, which can be thought of as a time like Mueller Regge expansion, the normality and isospin relation remain the same and the main difference lies in the transverse distributions.

In conclusion, we would like to thank those few who have actually read through to this point for bearing with us.

Acknowledgement

We wish to thank V. Rittenberg for discussions of branching models.

References

1. G. Kramer, J. Uretsky and T. F. Walsh; Phys. Rev. D3, 719 (1971)
J. Layssac, F. M. Renard; Nuovo Cim. 6, 134 (1971)
2. N. S. Craigie and K. D. Rothe; CERN preprint TH-1821 (Nuclear Physics, in print)
3. N. S. Craigie and K. D. Rothe; CERN preprint TH-1822 (Nuclear Physics, in print)
4. N. Cabibbo and R. Gatto; Phys. Rev. 124, 1577 (1961)
5. J. D. Bjorken; Proceedings of the 6th Int. Conf. on Electron and Photon Interactions. Ed. H. Rollnik and W. Pfeil, North-Holland (1974)
6. The precise form of Φ depends on the definition of $F(s, \omega)$; cf. The Appendix to II.
7. P. Zerwas and T. F. Walsh; Nuclear Physics B77, 494 (1974)
T. F. Walsh; Rutherford Meeting on Deep Inelastic Phenomena, May 4-5, 1974 (unpublished)
8. J. Ellis; Rutherford Meeting on Deep Inelastic Phenomena, May 4-5, 1974 (CERN, preprint 1880)
9. A. I. Sanda; NAL-Pub-74/16-THY
G. Schierholz and M. Schmidt (unpublished)
10. C. H. Llewellyn-Smith, IX Rencontre de Mariond, March 1974 (CERN preprint TH-1849)
11. L. Caneschi and A. Schwimmer; Phys.Lett. 33B, 577 (1970)
E. Berger, D. Horn and G. H. Thomas; Phys.Rev. D7, 1412 (1973)
12. R.C.E. Devenish, K. Koller, D. Schiller and T. F. Walsh; DESY Preprint 74/26
13. S. Gasiorowicz; Elementary Particle Physics (Wiley, 1966)

14. M. Chaichain and S. Kitakado; Nuovo Cim. Lett. I, 331 (1973)
15. R. Kingsley; Nucl. Phys. B58, 195 (1973)
16. J. K. Percus; Combinatorial Methods. (Springer, 1971)
17. M. Greco and Y. Srivastawa; Nuovo Cim. 18A, 601 (1973)
18. R.C.E. Devenish, K. Koller, D. Schiller and T. F. Walsh
(unpublished)
19. G. Kramer and T. F. Walsh; Z. Physik 263, 361 (1973)
20. N. S. Craigie and G. Kramer; DESY preprint 74/25
(Nuclear Physics, in print)
21. N. S. Craigie, J. Körner and G. Kramer; Nucl. Phys. B68, 509 (1974)
22. R. Kingsley; Princeton Preprint (1974)
23. R. Gatto and G. Preparata; Nuclear Physics B67, 362 (1973)
24. D. H. Scott; Nuovo Cimento 21A, 1 (1973)
25. A. M. Polyakov, JETP 32, 296 (1971), JETP 33, 850 (1971)
26. N. S. Craigie (in preparation)
27. S. J. Orfannidis and V. Rittenberg; Phys. Rev. Lett. 33, 455 (1974);
Rockefeller University Report No. COO-2232B-54 (unpublished).

Figure Captions

- Fig.1 The decay chain.
- Fig.2 The integral equation for $\rho(s)$.
- Fig.3 The integral equation for one particle inclusive production.
- Fig.4 The integral equation for two particle inclusive production.
- Fig.5 The decay chain with two states ρ and A .
- Fig.6 Sketch of the polynomial $P(\lambda)$.
- Fig.7a The two-particle inclusive driving term near $\omega_1 = 1$.
- Fig.7b Diagram for single-particle inclusive electroproduction.
- Fig.8a The crossed channel six-point function, in which we have indicated the partial wave decompositions of the $\pi\gamma$ channels with channel invariants t_1 and t_2 .
- Fig.8b The time-like Mueller Regge diagram, which we have assumed can be got from Fig.8a by crossing.
- Fig.9a,b
Diagrams for two-particle charge correlations with $\omega_1 \approx 1$.
- Fig.10 Qualitative picture of the distributions in $\tilde{\omega}_2 = \text{sign}(\cos\theta)\omega_2$ for a pion of definite charge at $\omega_1 \approx 1$.
- Fig.11a The equation describing the cascade with non-linear terms.
- Fig.11b The two pronged contribution.
- Fig.11c The three pronged interference term.
- Fig.11d An interference term involving a single pion.
- Fig.12a A reduced rapidity plot of the one-particle distribution for the chain emission model for two very large values of Q^2 .
- Fig.12b The corresponding plot expected for the parton model.
- Fig.12c The corresponding plot for branching models.

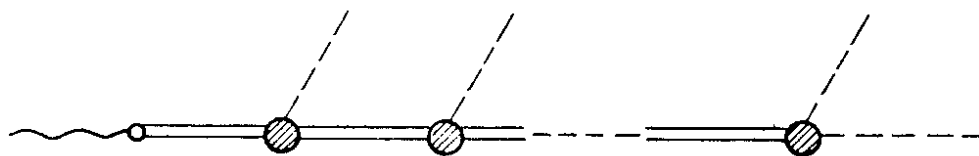


Fig.1

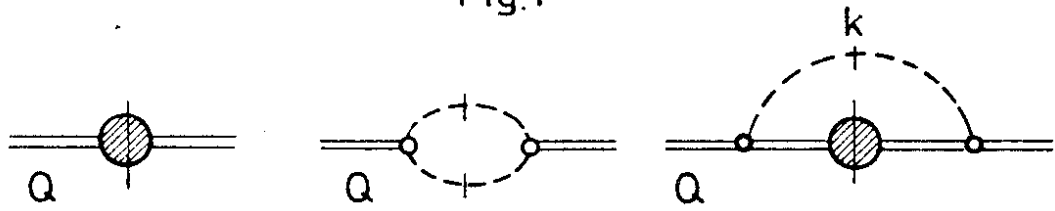


Fig.2

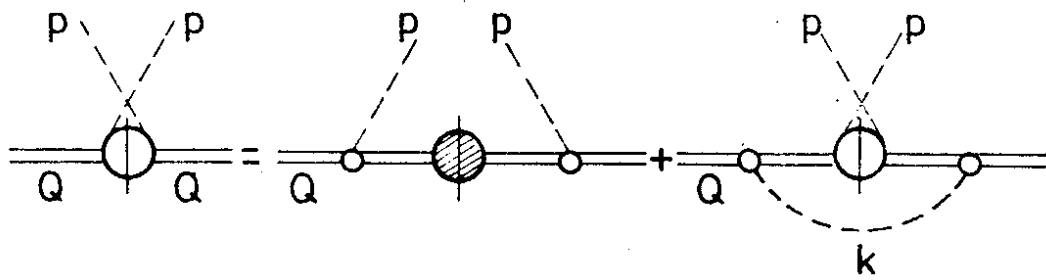
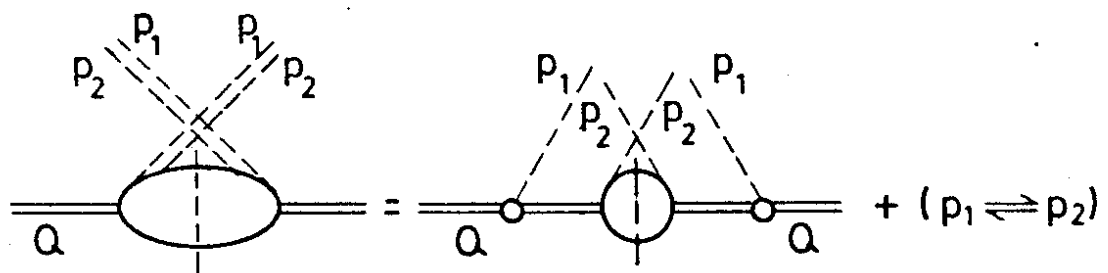
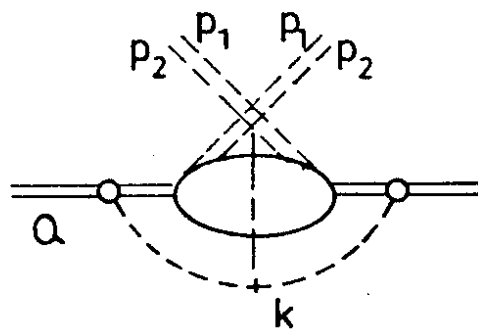


Fig.3



a)



b)

Fig.4

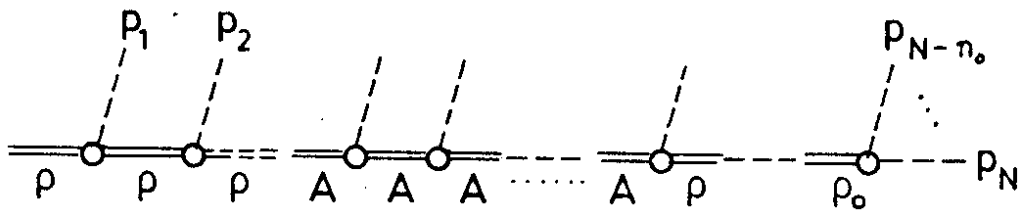


Fig.5

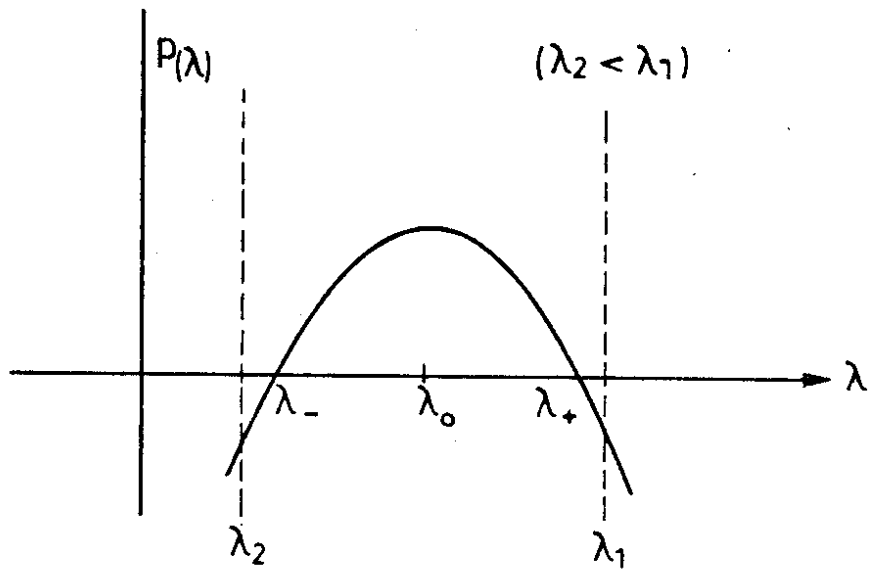
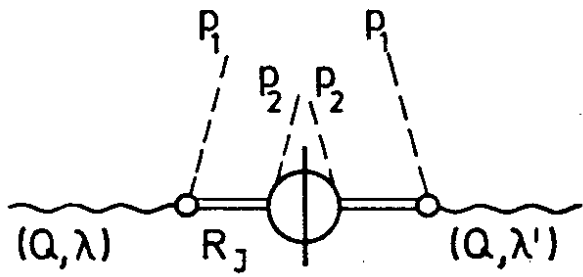
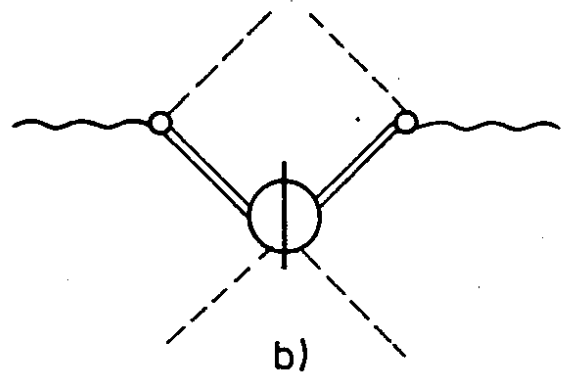


Fig.6

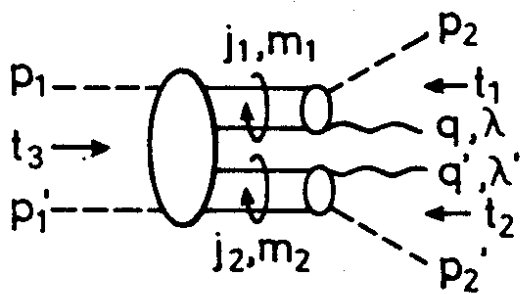


a)

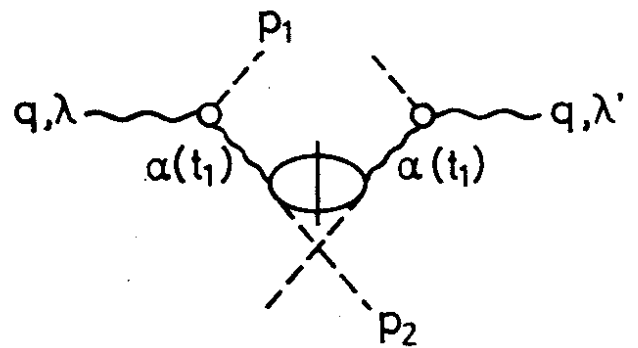


b)

Fig. 7

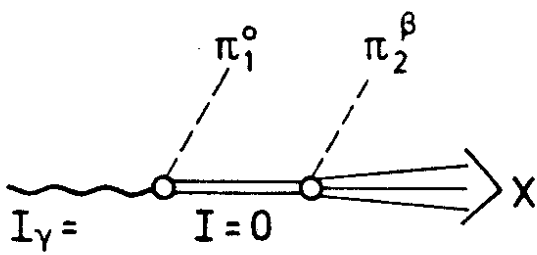


(a)

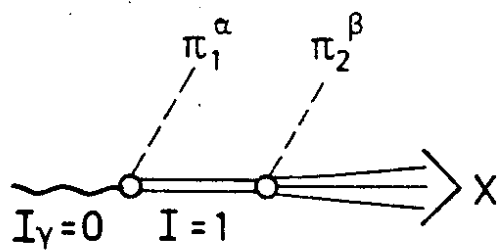


(b)

Fig. 8

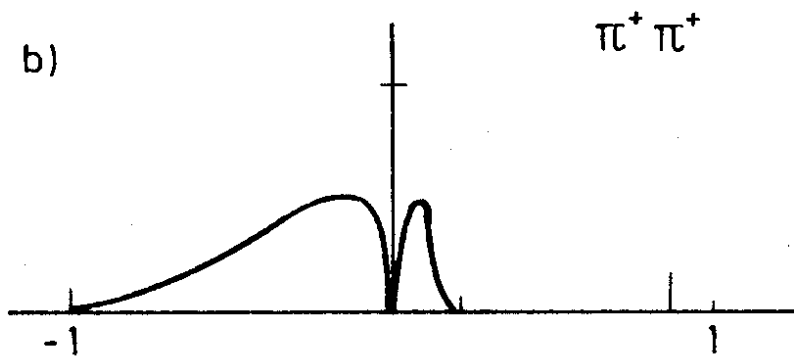
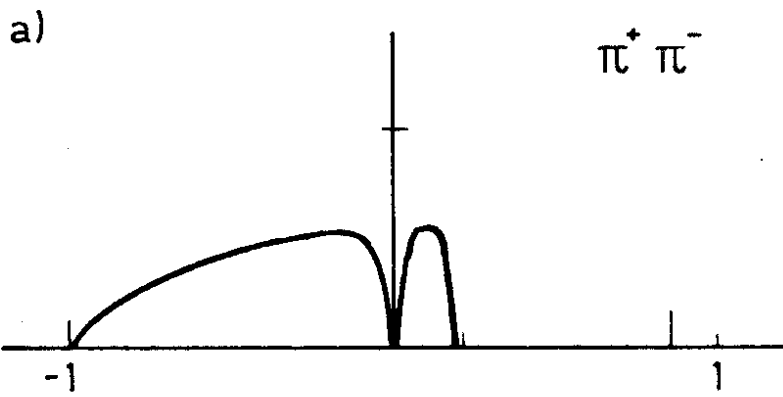
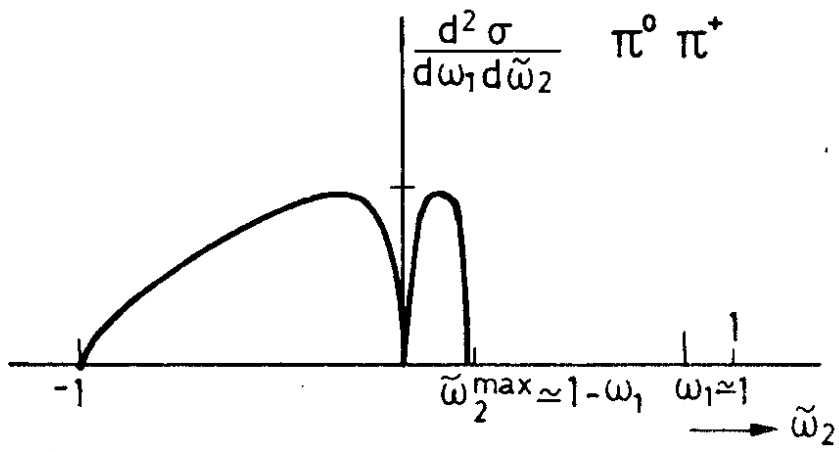


a)



b)

Fig 9



c)

Fig. 10

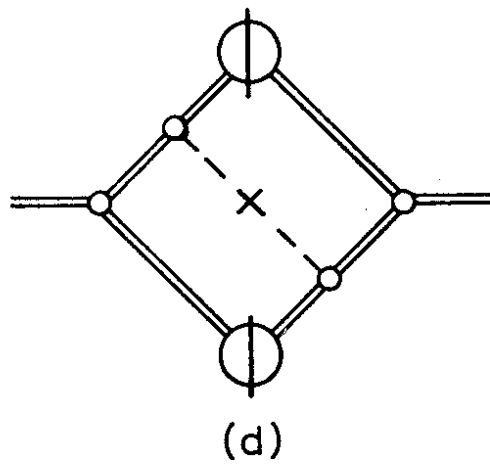
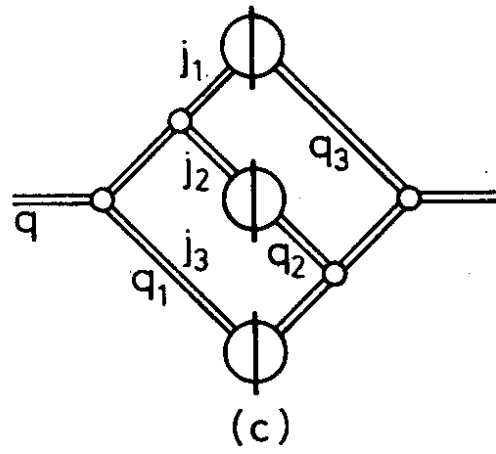
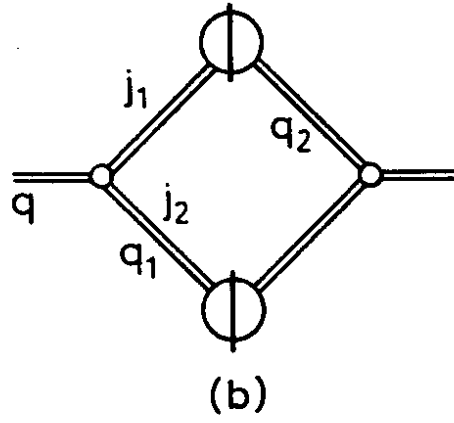
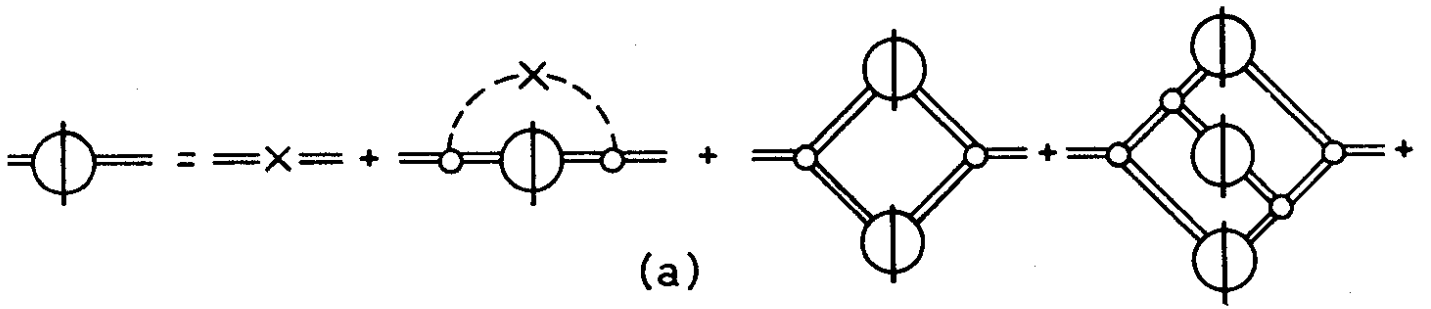


Fig. 11

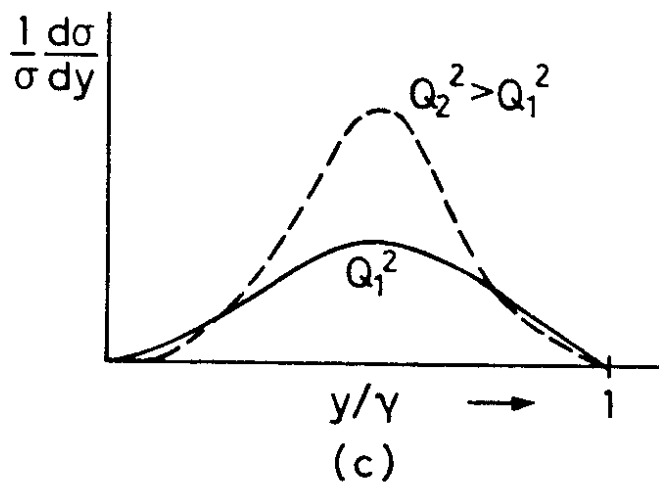
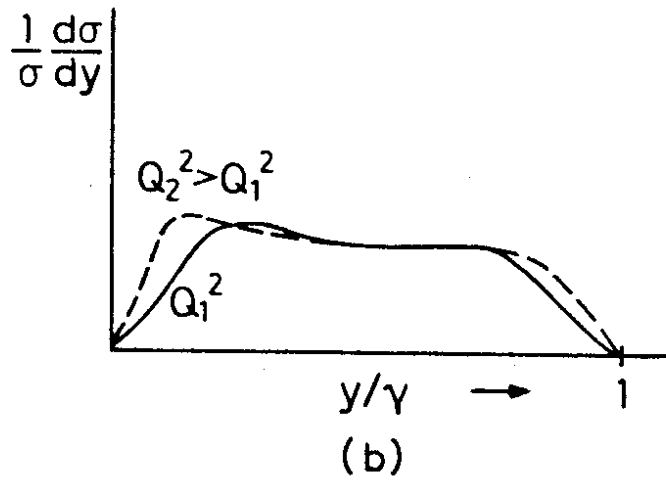
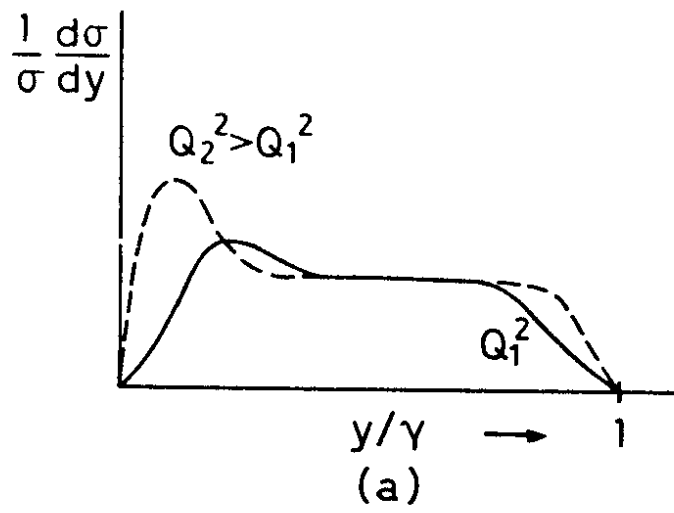


Fig. 12